

UC Irvine

UC Irvine Previously Published Works

Title

Activation of the NLRP3 Inflammasome Is Associated with Valosin-Containing Protein Myopathy.

Permalink

<https://escholarship.org/uc/item/8cj333w8>

Journal

Inflammation, 40(1)

ISSN

0360-3997

Authors

Nalbandian, Angèle
Khan, Arif A
Srivastava, Ruchi
[et al.](#)

Publication Date

2017-02-01

DOI

10.1007/s10753-016-0449-5

Copyright Information

This work is made available under the terms of a Creative Commons Attribution License, available at <https://creativecommons.org/licenses/by/4.0/>

Peer reviewed



Published in final edited form as:

Inflammation. 2017 February ; 40(1): 21–41. doi:10.1007/s10753-016-0449-5.

Activation of the NLRP3 Inflammasome is Associated with Valosin Containing Protein Myopathy

Angèle Nalbandian^{1,2,‡}, Arif A. Khan¹, Ruchi Srivastava¹, Katrina J. Llewellyn², Baichang Tan², Nora Shukr¹, Yasmin Fazli¹, Virginia E. Kimonis^{2,§}, and Lbachir BenMohamed^{1,3,4,‡,§}

¹Laboratory of Cellular and Molecular Immunology, Gavin Herbert Institute, University of California Irvine, School of Medicine, Irvine, CA 92697

²Division of Genetics and Genomics Medicine, Department of Pediatrics, University of California, Irvine, CA 92697

³Department of Molecular Biology & Biochemistry, University of California Irvine, School of Medicine, Irvine, CA 92697

⁴Institute for Immunology; University of California Irvine, School of Medicine, Irvine, CA 92697

Abstract

Aberrant activation of the NOD-like receptor (NLR) family, pyrin domain-containing protein 3 (NLRP3) inflammasome triggers a pathogenic inflammatory response in many inherited neurodegenerative disorders. Inflammation has recently been associated with Valosin Containing Protein (VCP)-associated diseases, caused by missense mutations in the *VCP* gene. This prompted us to investigate whether NLRP3 inflammasome plays a role in VCP-associated diseases, which classically affects the muscles, bones and brain. In this report, we demonstrate: (i) an elevated activation of the NLRP3 inflammasome in VCP myoblasts, derived from induced pluripotent stem cells (iPSCs) of VCP patients, which was significantly decreased following *in vitro* treatment with the MCC950, a potent and specific inhibitor of NLRP3 inflammasome; (ii) a significant increase in the expression of NLRP3, Caspase 1, IL-1 β and IL-18 in the quadriceps muscles of VCP^{R155H/+} heterozygote mice, an experimental mouse model that has many clinical features of human VCP-associated myopathy; (iii) a significant increase of number of IL-1 β ⁽⁺⁾F4/80⁽⁺⁾Ly6C⁽⁺⁾ inflammatory macrophages that infiltrate the muscles of VCP^{R155H/+} mice; (iv) NLRP3 inflammasome activation and accumulation IL-1 β ⁽⁺⁾F4/80⁽⁺⁾Ly6C⁽⁺⁾ macrophages positively correlated with high expression of TDP-43 and p62/*SQSTM1* markers of VCP pathology in damaged muscle; (v) treatment of VCP^{R155H/+} mice with MCC950 inhibitor suppressed activation of NLRP3 inflammasome, reduced the F4/80⁽⁺⁾Ly6C⁽⁺⁾IL-1 β ⁽⁺⁾ macrophage infiltrates in the muscle and significantly ameliorated muscle strength. Together, these results suggest: (i) NLRP3 inflammasome and local IL-1 β ⁽⁺⁾F4/80⁽⁺⁾Ly6C⁽⁺⁾ inflammatory macrophages contribute to pathogenesis of VCP-associated myopathy; and (ii) identified MCC950 specific inhibitor of the

[‡]Corresponding Authors: Angèle Nalbandian, Ph.D., Division of Genetics and Metabolism, Department of Pediatrics, University of California Irvine. a.nalbandian@uci.edu; Lbachir BenMohamed, Ph.D., Laboratory of Cellular and Molecular Immunology, Gavin Herbert Institute, University of California Irvine, lbenmoha@uci.edu.

[§]This work is supported by Public Health Service research grants from National Institutes of Health/NIAMS R56AR066970 (VEK) and EY14900, EY019896 and EY024618 (LBM).

Conflict of interest: The authors have declared that no conflict of interest exists.

NLRP3 inflammasome with promising therapeutic potential for the treatment of VCP-associated myopathy.

INTRODUCTION

The NLRP3 inflammasome is a multiprotein complex involving Caspase-1 and NLRP3, critical components of the innate immune system, which serve as a molecular platform mediating Caspase-1 activation and secretion of biologically active interleukin-1 beta (IL-1 β) [1–5]. Activation of the NLRP3 inflammasome results in processing of inactive pro-caspase-1 into an active cysteine-protease enzyme, Caspase-1. Subsequently, Caspase-1 induces the maturation and secretion of powerful proinflammatory IL-1 β cytokines, which in turn activate expression of other immune genes and recruitment of innate immune cells to damaged inflamed tissues.

The triggering of innate immune signaling pathways - in particular, the NOD-, LRR- and pyrin domain-containing 3 (NLRP3) inflammasome - by aberrant host proteins is emerging as a crucial component of diverse neurodegenerative diseases (reviewed in [6]). Particularly the activation of the NLRP3 inflammasome has been linked to the pathogenesis of several neurodegenerative disorders, including arthritis, silicosis, atherosclerosis and Alzheimer's disease [1, 3, 4, 6–12]. Monocytes co-expressing NLRP3 inflammasome was significantly increased in Alzheimer's disease (AD) [7]. However, the contribution of NLRP3 inflammasome in the myopathy associated to aberrant host Valosin Containing Protein (VCP), a disease that is caused by mutations in the VCP gene [13–16], which affects the muscle, bone and brain has not been explored. Patients with VCP-associated disease exhibit progressive proximal limb girdle muscular weakness and eventually die prematurely, around 40–50 years of age, from progressive muscle weakness and cardiac/respiratory failure [14, 17]. The clinical inflammatory hallmark of VCP-associated diseases, together with our recent finding that muscle wasting in VCP disease is associated with an increase in inflammatory cytokines [18], prompted us to investigate the role of NLRP3 inflammasome in VCP-associated myopathy.

Induced pluripotent stem cells (iPSCs) are adult cells that have been genetically reprogrammed to an embryonic stem cell-like state by being forced to express genes and factors important for maintaining the defining properties of embryonic stem cells (as reviewed in [19, 20]). Human iPSCs express stem cell markers and are capable of generating cells characteristic of all three germ layers (i.e. the ectoderm, the mesoderm, and the endoderm). Generation of skeletal muscle cells from iPSCs as an *in vitro* model and for therapy of muscular dystrophies has recently been reported [20]. Three VCP-associated iPSC cell lines harboring the R155H mutation and three control cell lines were used [19, 20].

In the present study, we hypothesized that: (i) aberrant host VCP protein leads by a yet-to-be-determined mechanism to activation of the NLRP3 inflammasome system in VCP patients thereby contributing to the muscle wasting; and (ii) strategies targeting the activation NLRP3 inflammasome could be useful in the therapy of VCP-associated myopathy. We report, for the first time: (i) a high activation of the NLRP3 inflammasome in

myoblasts, derived from induced pluripotent stem cells (iPSCs) of VCP patients, which was significantly decreased following *in vitro* treatment with the MCC950 compound, a potent NLRP3 inflammasome inhibitor. For practical and ethical reasons, human samples from muscles, bones and brains of VCP patients are limited resources, making it difficult to study the involvement of NLRP3 inflammasome in VCP-associated diseases in humans. Thus, we generated a novel VCP^{R155H/+} heterozygote mouse model that has many features typical of human VCP-associated disease including progressive muscle wasting, bone and brain pathologies, at approximately 12–15 months of age. Compared to age- and sex-matched wild type littermates, both the muscles and the bones of VCP^{R155H/+} heterozygote mice displayed: (i) a significant increase in the expression of NLRP3, Caspase 1 and IL-1 β in the quadriceps muscles; (ii) an increase in active macrophages in bones and muscles where they produced iNOS and IL-1 β inflammatory mediators; (iii) the level of NLRP3 inflammasome activation, the size of iNOS- and IL-1 β -producing inflammatory macrophages infiltrating damaged muscle of VCP^{R155H/+} heterozygote mice positively correlated with the severity of muscle wasting; (iv) treatment of VCP^{R155H/+} heterozygote mice with MCC950 inhibitor reversed the activation of NLRP3 inflammasome associated with a significant regression in muscle and brain pathologies.

Together, these results: (i) point at a novel inflammatory mechanism, whereby activation of the NLRP3 inflammasome occurs specifically in the muscle and the bone and contributes to pathogenesis of VCP-associated myopathy; (ii) delineate the quantitative and qualitative features of inflammatory responses associated with VCP-associated myopathy in both human and mice; and (iii) point to the NLRP3 Inflammasome cascade and inflammatory macrophages in the muscle as novel key players in the pathogenesis of VCP-associated myopathy.

MATERIALS AND METHODS

Ethics Statement

This study was carried out in strict accordance with the recommendations and procedures outlined in the IRB (#2009-1005) for patients and Guide for the Care and Use of Laboratory Animals of the National Institutes of Health under Assurance Number A3873-1. Experiments were conducted with the approval of the Institutional Animal Care and Use Committee (*IACUC Protocol #2007-2716-2*) of University of California-Irvine (Irvine, CA). Animals were housed at the University of California-Irvine vivarium and maintained as previously described [21]. All efforts were made to minimize suffering. Mouse genotyping was performed at Transnetyx Company, Inc. (Cordova, TN).

In vitro studies in induced pluripotent stem cells (iPSCs)-derived VCP patient myoblasts

Three VCP-associated iPSC cell lines harboring the R155H mutation and three control cell lines have been used. Control and VCP patient iPSC-derived myoblasts were cultured at 37°C in a humidified chamber with skeletal muscle induction medium (SkIM: high-glucose DMEM supplemented with 10% fetal calf serum (FCS; Thermo Fisher Scientific, Carlsbad, CA), 5% horse serum (HS; Sigma-Aldrich, St. Louis, MO), non-essential amino acids (Thermo Fisher Scientific), and 100 mM 2-mercaptoethanol) for 7 days, as we recently

described. **MCC950 Treatment:** Control and patient iPSC-derived control myoblasts (Day 49) were treated with MCC950 drug, an NLRP3 inhibitor, (Sigma Aldrich, St. Louis, MO) either at 0 μ M or 10 μ M and stained with anti-NLRP3, -TDP-43, -IL-18, -IL-1 β and -Caspase 1 (p10 and p20) antibodies. Cell lysates of the VCP patient and control myoblasts were prepared using NE-PER Nuclear and Cytoplasmic Extraction Kit (Thermo Scientific). Protein concentrations were determined using the Nanodrop and separated on Bis-Tris 4–12% NuPAGE gels (Thermo Fisher Scientific). Expression levels of proteins were analyzed by Western blotting using the following antibodies: NLRP3, IL-1 β , IL-18, Caspase 1 (cleaved p10 and p20) inflammatory mediators and correlate with loss of muscle function. Equal protein loading was confirmed by staining with the β -actin antibody (1:20,000 dilutions; mouse monoclonal anti- β -actin antibody). Further analysis was performed by Fluorescence-activated cell sorting (FACS) (Stem Cell Core Facility, University of California-Irvine, Irvine, CA) on either the untreated or treated VCP patient myoblasts with the aforementioned antibodies (Abcam, Cambridge, MA).

MCC950 Treatment: In Vitro and In Vivo Experimental Design in VCP^{R155H/+} mice

In vitro: Mouse primary myoblasts harvested from wild type (WT) and VCP^{R155H/+} heterozygote quadriceps muscles were cultured in Dulbecco's MEM supplemented with skeletal mix including 15% fetal calf serum at 37°C in a humidified chamber for three days. ***In vivo:*** Age- and sex-matched (12- and 24-months-old) VCP^{R155H/+} heterozygote and wild type mice (controls) were used for this investigation. Cohorts of mice were sacrificed and quadriceps muscles, brains, and bones were harvested for immunological and biochemical analyses. After gross examination, organs were washed with phosphate-buffered saline (PBS; pH 7.4) and cell suspensions were prepared for FACS and biochemical analyses. In addition, quadriceps muscles were flash frozen and bone and brains were 4% neutral-buffered formalin fixed for histological and immuno histochemical analyses as previously described [21]. ***MCC950 treatment:*** Mice were administered 30-mg/kg MCC950 treatment by oral gavage three times a week for one month and sacrificed to analyze the NLRP3 inflammasome pathway mediators and 'classical hallmarks of VCP pathology'. These experiments are representative of triplicates ($n = 8$ mice per group). ***In vitro:*** Wild type and VCP^{R155H/+} heterozygote myoblasts were harvested and treated with the NLRP3 inhibitor MCC950 drug, at either 0 μ M or 10 μ M concentrations and stained with mAbs specific to NLRP3, TDP-43, IL-18, IL-1 β and Caspase 1 (cleaved p10 and p20).

Measurements of weight and muscle strength

Muscle strength of the forelimbs of VCP^{R155H/+} heterozygote and WT mice was measured by a Grip Strength Meter apparatus (TSE Systems GmbH, Hamburg, Germany), as previously described [22–25]. Briefly, mice were held from the tip of the tail above the grid and gently lowered down until the front paws grasped the grid. Hind limbs were kept free from contact with the grid. The animal was brought to an almost horizontal position and pulled back gently, but steadily until the grip was released. The maximal force achieved by the animal was recorded.

Flow Cytometry Analysis (FACS)

To demonstrate the infiltration of inflammatory immune cells of the 24-month old VCP^{R155H/+} heterozygote and wild type (WT), we performed FACS analysis of quadriceps muscles, brains, and bones. Muscle, brain and bone lysates were harvested and levels of inflammasome activation and the amount of local pro-inflammatory mediators were determined from treated versus untreated mice. For this, cell suspensions from quadriceps muscles, brains and bones were analyzed by flow cytometry after staining with fluorochrome-conjugated and mouse-specific monoclonal antibodies (MAbs). The following anti-mouse antibodies were used: CD11b (clone M1/700)-PE, CD11c (clone HL3)-APC (BD Biosciences, San Jose, CA); Ly-6C (clone HK1.4)-PE-Cyanine7, iNOS (clone CXNFT)-AF488, (eBioscience, San Diego, CA); Ly-6G (clone 1A8)-AF700, F4/80 (clone BM8)-PE/Cy7 (BioLegend); IL-18 (clone [17H18L16]) (ThermoFisher Scientific); IL-1 β (clone B122) (Abcam), p62/*SQSTM1* (clone [EPR4844]) (Abcam), NLRP3 (clone [Nalpy3-a]) (Abcam), TDP-43 (clone [3H8]) (Abcam), Caspase 1 (ThermoFisher Scientific), LC3B (clone [5H12]) (Abcam), Bik (Abcam), BAK (clone [Y164]) (Abcam), and BAD (clone [Y208]) (Abcam). For surface staining, MAbs against various cell surface markers were added to a total of 1×10^6 cells in phosphate-buffered saline containing 1% FBS and 0.1% sodium azide (fluorescence-activated cell sorter [FACS] buffer) and left for 45 min at 4°C. After washing with the FACS buffer, cells were permeabilized for 20 min on ice using the TF Cytofix/Cytoperm buffer (BD Biosciences) and then washed twice with Perm/Wash buffer (BD Bioscience). Intracellular and/or intra-nuclear transcription factor staining MAbs were then added to the cells and incubated for 45 min on ice in the dark. Cells were washed again with Perm/Wash and FACS buffer and fixed in PBS containing 2% paraformaldehyde (Sigma-Aldrich). For each sample, 200,000 total events were acquired on a BD LSRII. Antibody capture beads (BD Biosciences) were used as individual compensation tubes for each fluorophore in the experiment. To define positive and negative populations, we employed fluorescence-minus controls for each fluorophore used in this study, when initially developing staining protocols. In addition, we further optimized gating by examining known negative cell populations for background level expression. Data analysis was performed using FlowJo version 9.9 (TreeStar, Ashland, OR). Statistical analyses were done using GraphPad Prism version 5 (GraphPad, La Jolla, CA).

Histological Staining

Eight micron sections from the 12-month and 24-month-old VCP^{R155H/+} heterozygote and WT quadriceps muscles, brains, and bones were stained by standard hematoxylin and eosin techniques for histological analysis to capture infiltration, as described above. Sections were mounted with Permount and visualized by light microscopy using an AxioVision image capture system (Carl Zeiss, Jena, Germany) at either 20 \times , 40 \times and/or 63 \times magnifications.

Immunohistochemical Analysis

For immunohistochemical (IHC) analysis, sections were stained with Caspase (1:3,000 dilution; rabbit monoclonal Caspase 1 antibody), NLRP3 (1:2,000 dilution; rabbit polyclonal NLRP3 antibody), TDP-43 (1:3,000 dilution; rabbit polyclonal anti-TDP-43 antibody), IL-18 (1:3,000 dilution; rabbit polyclonal anti-IL-18 antibody) and IL-1 β (1:3,000 dilution;

rabbit polyclonal anti-IL-1 β antibody) and mounted as previously described [21]. Cluster of Differentiation 68 (CD68), a glycoprotein which binds to low density lipoproteins was used to detect expression on monocytes and macrophages. Sections from the quadriceps muscles, brains, and bones were stained and analyzed by fluorescence microscopy using an AxioVision image capture system (Carl Zeiss), as previously described [26].

Western Blot Analysis

For Western blot analysis, 12- and 24-month old wild type and VCP^{R155H/+} heterozygote quadriceps muscles were harvested and extracted using the NE-PER Nuclear and Cytoplasmic Extraction Kit (Thermo Fisher Scientific). Protein concentrations were determined using the Nanodrop and separated on Bis-Tris 4–12% NuPAGE gels (Thermo Fisher Scientific). Expression levels of proteins were analyzed by Western blotting using NLRP3 (1:3,000 dilution), TDP-43 (1:3,000 dilution), IL-1 β (1:3,000 dilution), IL-18 (1:3,000 dilution), Caspase 1 (1:3,000 dilution; cleaved p10 and p20) inflammatory mediators and correlate with loss of muscle function. These antibodies were previously validated in our most recent publications [21, 26, 27]. All antibodies were purchased from Abcam (Cambridge, MA). Equal protein loading was confirmed by β -actin antibodies (1:20,000 dilution; mouse monoclonal anti- β -actin) staining. These experiments are representative of triplicates.

Statistical analyses

Data for each assay were compared by analysis of variance (ANOVA) and Student's *t*-test using Graph Pad Prism 5 software (San Diego, CA). Differences between the groups were identified by ANOVA, Mann-Whitney tests and multiple comparison procedures, as previously described [28]. Data are expressed as the mean \pm SD. Results were considered statistically significant at $p < 0.05$.

RESULTS

1. NLRP3 inflammasome signaling pathway is activated in myoblasts derived from patients with VCP disease

We first generated myoblasts from iPSCs-derived from either VCP patients (*VCP myoblasts*) or from healthy controls (*healthy myoblasts*) and stained them with monoclonal antibodies (mAbs) specific to human TAR DNA-binding protein 43 (TDP-43), a marker that resides in the nucleus and translocates during muscle and brain pathological states [29–32], NACHT, LRR, and PYD domains-containing protein 3 (NLRP3), IL-18, IL-1 β and cleaved activated forms of Caspase 1 (p10 and p20). As shown in *left two panels* of Fig. 1A, using immunocytochemistry we observed an increase in TDP-43, a 'classic' hallmark of VCP pathology, (which usually resides in the nucleus and is translocated to the cytoplasm during a pathological state), NLRP3, IL-18, Caspase 1 and IL-1 β in the VCP myoblasts as compared to the healthy myoblasts. Significant increases in the levels of IL-18, IL-1 β and activated caspase 1 (cleaved p10 and p20 forms) were confirmed by Western blot in *VCP myoblasts* as compared to the *healthy myoblasts* ($P < 0.05$, *left two panels* of Figs. 1B and 1C). These results demonstrated an activation of the NLRP3 inflammasome signaling

pathway in the myoblasts from patients with VCP disease, implying the NLRP3 Inflammasome as a novel player in the pathogenesis of VCP-associated myopathy.

2. Activation of NLRP3 inflammasome is significantly decreased in human VCP myoblasts following *in vitro* treatment with the MCC950 inhibitor

We next sought to determine whether the activation of NLRP3 inflammasome, detected in human VCP myoblasts, can be reversed following *in vitro* treatment with MCC950 (i.e. $C_2O_4H_2N_2NaO_5S$), a potent, selective and small-molecule inhibitor of NLRP3 [33]. Myoblasts were generated from iPSCs derived from either VCP patients or from control healthy donors, as described above. Myoblasts were then either left untreated (0 μ M or VCP untreated) or treated for 16 hours with 10 μ M of MCC950 inhibitor (*VCP treated*) and then stained with mAbs specific to human TDP-43, NLRP3, IL-18, IL-1 β and Caspase 1, as described above. As shown in *right two panels* of Fig. 1A a significant decrease was observed by immunocytochemistry for TDP-43, NLRP3, IL-18, IL-1 β and Caspase 1 in treated vs. untreated VCP myoblasts (0 μ M vs. 10 μ M). To determine whether Caspase 1 activation was blocked following treatment with MCC950 inhibitor, using Western blotting, we stained for cleaved forms of Caspase 1 (cleaved p10 and p20). MCC950 inhibitor prevented Caspase 1 activation, the effector of the NLRP3 inflammasome, induced in VCP myoblasts (*right two panels* of Figs. 1B and 1C). Moreover, results from the Western blotting confirmed that the level of TDP-43, NLRP3, IL-18 and IL-1 β proteins were downregulated following treatment with the MCC950 inhibitor (*right panels* of Figs. 1B and 1C).

To ascertain inhibition of NLRP3 inflammasome occurs in live VCP myoblasts following MCC950 inhibitor treatment, we compared the levels of the expression of NLRP3, Caspase 1, IL-1 β and IL-18 from treated and untreated VCP myoblasts using flow cytometry. Myoblasts were generated from iPSCs derived from either VCP patients or from control healthy donors, as described above. Myoblasts were then left either untreated (0 μ M or VCP untreated) or treated for 16 hours with 10 μ M of MCC950 inhibitor (*VCP treated*) and then stained with mAbs specific to human NLRP3, Caspase 1, IL-1 β and IL-18. In addition, we also stained for anti-apoptotic markers, namely, Bcl-2-Interacting Killer (BIK), Bcl-2-antagonist/killer (BAK), and Bcl-2-associated death promoter (BAD). As shown in Fig. 2A, following treatment of live VCP myoblasts with the MCC950 inhibitor, a significant decrease was detected in the levels of NLRP3 (MFI treated vs. untreated VCP myoblasts 29974 vs. 19701, respectively), IL-1 β (MFI treated vs. untreated VCP myoblasts 17976 vs. 11982, respectively), and IL-18 (MFI treated vs. untreated VCP myoblasts 13319 vs. 9440, respectively). Interestingly, following treatment of live VCP myoblasts with the MCC950 inhibitor, a significant decrease was detected in the levels of anti-apoptotic markers, BIK (MFI treated vs. untreated VCP myoblasts 3100 vs. 2279, respectively) and BAD (MFI treated vs. untreated VCP myoblasts 2287 vs. 1872, respectively) (Fig. 2B).

For practical and ethical reasons, human samples from muscle, bone and brain are limited resources, making it difficult to determine whether the NLRP3 inflammasome pathway is also activated in bones and brains with VCP-associated diseases. Thus, the remainder of the study was conducted using our unique VCP^{R155H/+} heterozygote experimental mouse

model, which features clinical characteristics that closely mimics human VCP-associated myopathy [27, 34, 35]. Altogether, these results from immunocytochemistry, Western blotting and flow cytometry corroborate to confirm activation of the NLRP3 inflammasome in human VCP myoblasts and that this activation can be significantly downregulated following *in vitro* treatment with the MCC950 Inhibitor.

3. A significant increase in the expression levels of Caspase 1, NLRP3, and IL-1 β in the quadriceps muscles of VCP^{R155H/+} heterozygote mice

To determine when, where (i.e. muscle, bone and/or brain) and how activation of the NLRP3 inflammasome leads to VCP-associated myopathy, we used our knock-in VCP^{R155H/+} heterozygote mouse model. Quadriceps femoris muscles, also known simply the quadriceps, are the great extensor muscle of the knee, forming a large fleshy mass that covers the front and sides of the femur. Similar to our human data reported above, we found that the NLRP3 inflammasome pathway was highly activated in the quadriceps femoris muscles of 2-year-old VCP^{R155H/+} heterozygote mice as compared to quadriceps femoris muscles of age- and sex-matched wild type control littermates ($P < 0.05$, *left two panels* of Fig. 3A, *left two panels* of Figs. 3B and 3C). We observed significant increases in the expression levels of NLRP3, IL-18, Caspase 1 and IL-1 β markers of inflammation associated with an increased and translocated expression level of TDP-43 („classic“ VCP pathology) in the quadriceps muscles of VCP^{R155H/+} heterozygote mice as compared to age- and sex-matched controls. In addition, we also detected increased levels of IL-18 and IL-1 β in VCP^{R155H/+} heterozygote mice as compared to age- and sex-matched WT control littermates (Fig. 3A, *left two panels*). Significant increases in the levels of NLRP3, induced nitric oxide synthase (iNOS), activated Caspase 1 (i.e. cleaved p10 and p20 forms), IL-1 β , and IL-18 were confirmed by Western blot in the quadriceps of VCP^{R155H/+} heterozygotes as compared to age- and sex-matched WT littermates (*left two panels* of Figs. 3B and 3C, $P < 0.05$).

Altogether, these results demonstrate that, similar to humans, NLRP3 inflammasome is activated in the quadriceps muscles of VCP^{R155H/+} heterozygote experimental mouse model. These findings confirm the NLRP3 inflammasome pathway as a novel player in the pathogenesis of VCP-associated myopathy.

4. Increased number of IL-1 β -producing inflammatory macrophages in damaged muscle and bones of VCP^{R155H/+} heterozygote mice

The NLRP3 inflammasome triggers IL-1 β secretion by myeloid cells in response to endogenous and exogenous danger signals (reviewed in [36]). Local IL-1 β subsequently triggers inflammatory cell recruitment to the site of injury [37–39]. The high levels of IL-1 β detected in muscle of VCP^{R155H/+} heterozygote mice prompted us to determine its cell source. Hematoxylin and eosin sections in Fig. 4A show significant cell infiltrates, likely comprised of macrophages and necrotic myocytes (immunostained with CD68 marker, a glycoprotein expressed on monocytes and macrophages; in parallel stained with Hematoxylin and eosin), in muscle of 2-year-old VCP^{R155H/+} heterozygote as compared to age- and sex-matched WT littermate mice.

We then compared the frequency of inflammatory macrophages, producing both IL-1 β , in the quadriceps muscles, bones, and brains of VCP^{R155H/+} heterozygote mice vs. age and sex-matched WT littermates using flow cytometry. Cell suspensions from quadriceps muscles, bones, and brains of 2-years-old VCP^{R155H/+} heterozygote and WT littermate mice were prepared and double-stained with anti-F4/80 and anti-LyC6 mAbs. F4/80 marker is expressed at high level on various types of macrophages. Ly6C is ideally suited for the detection of activated macrophages in inflammatory tissues. We found significantly higher percentages of F4/80⁺IL-1 β ⁺ macrophages infiltrating both the muscle and the bones of VCP^{R155H/+} heterozygote mice compared to age- and sex-matched WT littermates (Figs. 4B and 4C, $P = 0.04$ and $P = 0.02$, respectively) and higher numbers (Fig. 4D, $P = 0.02$). A 3-fold increase in F4/80⁺IL-1 β ⁺ macrophages was detected in the muscle of 2-year-old VCP^{R155H/+} heterozygote mice as compared to age- and sex-matched WT littermates (*not shown*). In contrast, no significant differences in the percentages (Figs. 4B and 4C) and numbers (Fig. 4D) of F4/80⁺IL-1 β ⁺ macrophages were detected in the brains of VCP^{R155H/+} heterozygote mice and their age- and sex-matched WT mice littermates ($P > 0.05$).

Moreover, we discovered a 2-fold increase in the percentages (Figs. 4E and 4F, $P = 0.01$) and numbers (Figs. 4G, $P = 0.03$) of Ly6c⁽⁺⁾IL-1 β ⁽⁺⁾ activated macrophages in the muscles of 2-year-old VCP^{R155H/+} heterozygote mice as compared to the muscle of their WT littermates. A significant increase of Ly6c⁽⁺⁾IL-1 β ⁽⁺⁾ activated macrophages was also detected in the bone, but not in the brain, of one-year-old VCP^{R155H/+} mice as compared to wild type mice (16.5% Ly-6C⁽⁺⁾IL-1 β ⁽⁺⁾ cells vs. 9.7% Ly-6C⁽⁺⁾IL-1 β ⁽⁺⁾ cells, respectively, $P < 0.04$). Altogether, these results suggest that the increase of the number of inflammatory IL1 β F4/80⁽⁺⁾Ly-6C⁽⁺⁾ macrophages in the damaged muscles and bones of VCP-associated myopathy might contribute to pathology in VCP^{R155H/+} heterozygote mice.

5. In vitro treatment of myoblasts from VCP^{R155H/+} heterozygote mice with MCC950 pharmacologic inhibitor reverses NLRP3 inflammasome activation and reduces markers of VCP pathology

We next sought to determine: (i) whether the activation of NLRP3 inflammasome detected in mouse VCP myoblasts can be reversed following *in vitro* treatment with MCC950, a potent pharmacological inhibitor that blocks canonical and non-canonical NLRP3 activation at nanomolar concentrations as previously described [33]; and (ii) whether reversing the activation of NLRP3 inflammasome will lead to improvement in muscle pathology.

Myoblasts were harvested from quadriceps muscles of age- and sex-matched VCP^{R155H/+} heterozygotes and healthy naive mice (wild type control) littermates, treated for 16 hours with 10 μ M MCC950 inhibitor and analyzed by FACS for signs of inflammation including the following markers: NLRP3, Caspase 1, IL-1 β and IL-18, as aforementioned. The level of expression of markers of pathology TDP-43 and p62/*SQSTM1* were also compared in parallel in treated vs. untreated VCP myoblasts. As shown in Figs 5A and 5C, compared to untreated VCP myoblasts, MCC950-treated VCP myoblasts exhibited significant decreases in the expression levels of NLRP3 (MFI 3708 vs. 5119, $P < 0.02$), Caspase 1 (MFI 580 vs. 1343, $P < 0.02$), IL-1 β (MFI 12957 vs. 19941, $P < 0.03$), and IL-18 (MFI 558 vs. 940, $P < 0.003$). Moreover, MCC950-treated VCP myoblasts exhibited a statistically significant

improvement in the pathology as judged by a decrease in TDP-43, a ‘hallmark of VCP pathology’ (which usually resides in the nucleus and is translocated to the cytoplasm during a pathological state) (Figs. 5A and 5C, MFI 2195 vs. 3562, treated VCP myoblasts versus untreated VCP myoblasts respectively, $P < 0.02$). The p62 protein, also known as *sequestosome 1 (SQSTM1)*, a ubiquitin-binding scaffold protein that co-localizes with ubiquitinated protein aggregates in many neurodegenerative and proteinopathy diseases such as VCP was also downregulated following MCC950 treatment (MFI 7857 vs. 23805, treated VCP myoblasts vs. untreated VCP myoblasts respectively, $P < 0.01$). In contrast, compared to untreated healthy myoblasts, MCC950-treated healthy myoblasts showed no statistical differences in the expression levels of markers for inflammation and pathology (Figs. 5B and 5D).

Altogether, these results indicate that *in vitro* treatment of mouse VCP myoblasts with the MCC950 inhibitor: (i) was efficacious in decreasing NLRP3 inflammasome mediators; (ii) this inhibition of NLRP3 inflammasome coincided with a decrease in TDP-43 and p62/*SQSTM1* markers of pathology; and (iii) since MCC950 specifically inhibits NLRP3, but not AIM2, NLRC4 or NLRP1 activation [33], the results confirm that NLRP3 inflammasome alone contributes to muscle VCP disease pathology.

6. Suppression of NLRP3 inflammasome activation, following treatment with MCC950 pharmacologic inhibitor, led to a significant amelioration of muscle strength in the VCP^{R155H/+} heterozygote experimental mouse model

So far, our results indicate that activation of the NLRP3 inflammasome and the subsequent increase in the number of local inflammatory IL1 β F4/80⁽⁺⁾Ly-6C⁽⁺⁾ macrophages in the quadriceps muscles and bones are associated with pathology in VCP^{R155H/+} heterozygote mice. However, it remains unknown whether activation of the NLRP inflammasome contributes to VCP disease *in vivo*. Thus, in a final experiment, we sought to determine: (i) whether *in vivo* treatment with MCC950 inhibitor would reverse the activation of the NLRP3 inflammasome pathway detected in the quadriceps muscles of VCP^{R155H/+} heterozygote mice; and (ii) whether MCC950-mediated reversion of NLRP3 inflammasome activation would improve skeletal muscle atrophy in VCP^{R155H/+} heterozygote mice.

Two groups of sex-matched 12-month and 18-month VCP^{R155H/+} heterozygotes mice received oral gavage of 30-mg/kg of MCC950 inhibitor for 4 consecutive weeks. Untreated age- and sex-matched VCP^{R155H/+} heterozygotes mice were used as controls. Muscle strength was also compared between MCC950 treated and untreated mice using muscle grips as previously described [27]. Grip strength in MCC950-treated 12-month old VCP^{R155H/+} mice was significantly higher than that in untreated mice ($p < 0.045$) (Table 1). Treated and untreated mice from both VCP^{R155H/+} and wild type group were sacrificed at the end of the 4 weeks treatment, and quadriceps, brains, and bones were harvested. Cell infiltrates were examined in hematoxylin and eosin sections of muscle harvested from VCP^{R155H/+} heterozygote and age- and sex-matched WT littermate mice.

The hematoxylin and eosin sections in Fig. 6A show a significant reduction in cell infiltrates in muscle of 2 years old VCP^{R155H/+} heterozygote following MCC950 treatment (i.e. muscle fiber size, central nuclei, fibrosis, vacuoles). Subsequently, the expression levels of markers

of inflammation NLRP3, Caspase 1, IL-1 β and IL-18 and of markers of pathogenicity TDP-43 and p62/*SQSTM1* were then compared in MCC950-treated and untreated groups using FACS, as described above.

As shown in Figs. 6B and 6C (*left panels*), MCC950 treatment resulted in a 3-fold decrease in expression of NLRP3 (MFI: 512 vs. 1583, treated vs. untreated, respectively, $P=0.02$), a 3-fold decrease in Caspase 1 (cleaved p10 and p20) (MFI: 731 vs. 1917, treated vs. untreated, respectively, $P=0.01$) and a 2-fold decrease in the pro-inflammatory IL-1 β cytokine (MFI: 2853 vs. 7046, treated vs. untreated, respectively, $P=0.03$). The decrease in these proinflammatory markers in MCC950-treated VCP^{R155H/+} heterozygotes mice was associated with: (i) a decrease in „hallmark markers of VCP pathology“, namely TDP-43 (MFI: 6364 vs. 15367, treated vs. untreated, respectively, $P=0.02$), and p62/*SQSTM1* (MFI: 845 vs. 1564, treated vs. untreated, respectively, $P=0.04$) (Figs. 6B and 6C (*right panels*)).

We next compared the percentages and numbers of inflammatory macrophages, producing IL-1 β in the quadriceps femoris muscles of MCC950-treated vs. untreated 2-year-old VCP^{R155H/+} heterozygote mice. For this, quadriceps muscles cell suspensions were triple-stained with anti-F4/80, anti-Ly6C⁽⁺⁾ and anti-IL-1 β mAbs. MCC950 treatment resulted in a significant decrease in the percentage (Fig. 6D, *left panel*) and numbers (Fig. 6D, *right panel*) of IL-1 β F4/80⁽⁺⁾ macrophages infiltrating the muscles quadriceps. Similarly, treatment of 2-year-old VCP^{R155H/+} heterozygote mice with MCC950 significantly reduced the percentage (Fig. 6E, *left panel*) and numbers (Fig. 6E, *right panel*) of IL-1 β ⁽⁺⁾Ly6C⁽⁺⁾ inflammatory macrophages infiltrating the muscles quadriceps.

Moreover, the decrease in the markers of inflammation NLRP3, Caspase 1, IL-1 β and IL-18 and of the markers of VCP pathogenicity TDP-43 and p62/*SQSTM1* and the decrease of numbers of inflammatory macrophages, producing IL-1 β and iNOS, in the quadriceps femoris muscles of MCC950-treated vs. untreated 2-year-old VCP^{R155H/+} heterozygote mice was associated with: (i) a significant amelioration of muscle strength ($P<0.05$) (Fig. 6H), as detected by grip strength analyses (Table 1) [27]. The MCC950-treated mice depicted an improvement of 50.3 ± 4.6 in muscle grip strength as compared to only 40.14% (± 3.2) the untreated VCP animals by the receiver operating characteristic (ROC) curve (Table 1 and Fig. 6H); (ii) a stable weight loss in treated compared to untreated VCP^{R155H/+} heterozygotes mice (Figs. 6F and 6G); and (iii) loss of limb quadriceps muscle mass observed in untreated VCP^{R155H/+} heterozygote mice compared to treated mice and is associated with inflammation Figs. 6H, 6I and 6J.

Altogether, these results demonstrate that treatment of VCP^{R155H/+} heterozygote mice with MCC950 inhibitor suppressed activation of NLRP3 inflammasome and reduced the number of F4/80⁽⁺⁾Ly6C⁽⁺⁾IL-1 β ⁽⁺⁾ macrophages in the muscle which was associated with a significant amelioration in muscle strength. The results confirm that the NLRP3 inflammasome and local IL-1 β ⁽⁺⁾F4/80⁽⁺⁾Ly6C⁽⁺⁾ macrophages as novel players in the pathogenesis of VCP-associated myopathy and identified the sulfonylurea MCC950 inhibitor of the NLRP3 inflammasome with promising therapeutic potential for the treatment of VCP-associated myopathy.

DISCUSSION

In the present study, we demonstrated NLRP3 inflammasome and IL-1 β ⁽⁺⁾F4/80⁽⁺⁾Ly6C⁽⁺⁾ inflammatory macrophages as novel players that contribute in the pathogenesis of VCP-associated myopathy, a disease that classically affects the muscles, bones and brains [17, 40]. The NLRP3 inflammasome cascade was highly activated in the muscles of patients with VCP disease and in muscles and bones of the VCP^{R155H/+} heterozygote mouse model of VCP-associated myopathy. Compared to age- and sex-matched wild type littermates, both the quadriceps muscles and bones, but not the brains, of 2-year-old VCP^{R155H/+} mice displayed: (i) increased numbers of inflammatory macrophages that produce pro-inflammatory IL-1 β and iNOS; (ii) increased activation of NLRP3 inflammasome; (iii) higher amount of activated caspase 1 (cleaved p10 and p20); and (iv) a positive correlation between the expression levels of bone and muscular inflammation, TDP-43 and p62/*SQSTM1* pathogenic markers and severity of muscle wasting. Moreover, suppression of NLRP3 inflammasome activation, following treatment of with MCC950 pharmacologic inhibitor, led to a significant amelioration of muscle strength in our VCP^{R155H/+} heterozygote experimental mouse model.

VCP-associated disease is a rare disorder with overlapping pathologies, caused by missense mutations within the *VCP gene*, classically affecting the muscle, bone and brain [41]. Patients with VCP-associated myopathy exhibit proximal limb girdle muscular weakness and eventually die, prematurely around 40–50 years of age from progressive muscle weakness, cardiomyopathy and respiratory failure. Both clinical and translational laboratory studies have demonstrated that chronic inflammation is associated with VCP-associated myopathy. Muscle pathology leads to an increase in autophagy markers such as *sequestosome 1* (p62/*SQSTM1*) [27, 42, 43]. The p62/*SQSTM1* interacts with the autophagic effector protein Light Chain 3 (LC3-I/II) to mediate the uptake of aggregated proteins [44, 45]. Inclusions seen in the muscles and brain of VCP patients contain ubiquitin, beta amyloid, p62/*SQSTM1* and TDP-43 ('classic' hallmark markers of VCP disease) are also observed in other neurodegenerative disorders, such as Alzheimer disease (AD) and more recently Amyotrophic Lateral Sclerosis (ALS), thus implicating common inflammatory pathways in their pathogenesis [46–50]. However, the precise etiopathogenetic inflammatory mechanisms linking VCP-associated myopathy remain to be elucidated, and the pathways that mediate this phenomenon are not fully characterized. It is likely that accumulation of "mutated pathogenic VCPs" in the cytosol of damaged muscle cells impair migration and clearance of damaged mitochondria, leading to an increase in the number of abnormal mitochondria on damaged muscle, which contribute to disease.

To our knowledge, this is the first report to implicate NLRP3 inflammasome in a VCP-associated myopathy. We found a significant increase in the expression of NLRP3, Caspase 1, IL-1 β and IL-18 in the quadriceps muscles of VCP^{R155H/+} heterozygote mice, an experimental mouse model that has many clinical features of human VCP-associated myopathy. Moreover, a significant increase of IL-1 β ⁽⁺⁾F4/80⁽⁺⁾Ly6C⁽⁺⁾ macrophages infiltrating the damaged quadriceps muscles and bones of VCP^{R155H/+} heterozygote positively correlated with high expression levels of TDP-43 and p62/*SQSTM1* markers of VCP pathology and with progressive muscle wasting. The release of Nitric Oxide Synthetase

(NOS) and Reactive Oxygen Species (ROS) from damaged muscular tissues together with stimulation of the NLRP3 inflammasome and increase in the number of local inflammatory IL-1 β ⁽⁺⁾F4/80⁽⁺⁾Ly6C⁽⁺⁾ macrophages might also contribute to local inflammation and damaged muscular tissue leading to VCP-associated myopathy.

The triggering of inflammatory responses initiated by inflammasomes is emerging as a crucial component that contribute to neurodegenerative disorders (reviewed in [6] and [10]). Activation of inflammasome pathways is responsible for activation of inflammatory processes, and can induce cell pyroptosis, a process of programmed cell death distinct from apoptosis [51, 52]. While four major types of inflammasomes are reported (i.e. NLRP1, NLRP3, NLRC4 and AIM2); the activation of NLRP3 pathway by aberrant host proteins appears to be a common step that contribute to tissue damage and to the development of diverse neurodegenerative disorders [6, 47, 53]. The NLRP3 inflammasome is a multiprotein complex involving Caspase 1, a critical component of the innate immune system, which serve as a molecular platform mediating secretion of biologically active pro-inflammatory IL-1 β and IL-18 [1–5]. Deregulated activation of NLRP3 has been linked to the pathogenesis of several acquired inflammatory disorders including gouty arthritis, silicosis, atherosclerosis, diabetes and Alzheimer's disease [1, 3, 4, 54, 55]. To the best of our knowledge, the present study is first to demonstrate the contribution of the NLRP3 inflammasome in VCP myopathy (Figs. 1 *thru* 6). It appears that the muscles and the bones, but not the brain, are the organs that were most involved in this inflammatory process observed in our experimental VCP^{R155H/+} heterozygote mouse model. Similarly, in humans, approximately 90% of affected VCP patients have muscle weakness while about half of affected VCP patients have Paget disease of bone characterized by abnormal rates of bone growth that can result in bone pain, enlargement and fractures [13, 14]. The similarity of our mouse and human results support VCP^{R155H/+} heterozygote mice, as a reliable experimental mouse model that has many clinical features of human VCP-associated myopathy. This mouse model can be used to speed up the process of pre-clinically assessing treatment strategies that are desperately needed to ameliorate VCP disease. While the present study focused on the effects of MCC950 compound on ameliorating muscle injury in VCP disease, future detailed studies will unravel the effects of MCC950 on other organs, such as the brains and the bones.

Moreover, the present study identified the sulfonylurea MCC950 inhibitor of the NLRP3 inflammasome as a promising therapeutic drug for the treatment of VCP-associated myopathy. Our pre-clinical study showed a significant amelioration of muscle strength in VCP^{R155H/+} heterozygote experimental mice that were given MCC950 orally, paving the way for future clinical trials. Several NLRP3 inflammasome inhibitors have been previously described, some of which show promise in the clinic (as reviewed in [56]). The specificity of the novel MCC950 compound, which specifically inhibits NLRP3, but not AIM2, NLRC4 or NLRP1 activation [33], together with its efficacy when given orally makes it an attractive therapy, both at the cost and practical levels compared to current protein-based treatments, which are given daily, weekly, or monthly by injection. Determining whether the NLRP3 inflammasome is associated with the onset and progression of VCP-associated diseases and the underlying mechanisms of how NLRP3 inflammasome becomes activated in VCP-associated diseases are certainly important goals, but remains beyond the scope of this study.

Nevertheless, the results in this report represent a good starting point for an innovative and complementary therapeutic target to reverse the detrimental consequences of inflammation in VCP-associated neuromuscular and neurodegenerative diseases.

The findings in this report point to a novel immune mechanism whereby dysfunctional protein homeostasis caused by *VCP* mutations leads, by a yet-to-be determined mechanism, activates the NLRP3 inflammasome cascade, specifically in the muscles and the bones. This may contribute to muscle wasting and to the pathogenesis of VCP-associated myopathy. Although sarcopenia (loss of muscle mass) observed in VCP-associated myopathy is associated with inflammation, so far the potential role of the NLRP3 inflammasome in muscle weakness and muscle production of inflammatory mediators has not yet been investigated. There is evidence that components of the inflammasome complex are upregulated in dysferlin-deficient human muscle, thus suggesting that skeletal muscle cells can actively participate in inflammasome activation [57]. This is a crucial point as recent studies have demonstrated that skeletal muscle cells produce and release cytokines (myokines) that act in an autocrine, paracrine, and/or endocrine manner to modulate metabolic and inflammatory processes. For example, we recently found significant differences in circulating levels of cytokines (TNF- α and EGF) in patients with VCP disease versus healthy control groups [18]. However, the interactions between local NLRP3 expression/activation and these myokines production as well as the effects of these interactions on muscle function remain yet to be investigated.

The NLRP3 inflammasome triggers interleukin-1 (IL-1) secretion by myeloid cells in response to endogenous and exogenous danger signals [36]. In this report, we discovered that IL-1 β was elevated in the muscles of both VCP patients as well as in VCP^{R155H/+} heterozygote experimental mouse model. F4/80⁽⁺⁾Ly6C⁽⁺⁾ macrophages infiltrating damaged muscle were identified as a major cell source of IL-1 β . Activation of the NLRP3 inflammasome pathway, which leads to production of inflammatory IL-1 β , appeared to correlate with loss of muscle strength in VCP^{R155H/+} heterozygote mice. Recent reports indicate that IL-1 β exerts a crucial role in the initiation and progression of the idiopathic inflammatory myopathies, a heterogeneous group of chronic disorders with predominant inflammation in muscle tissue, including dermatomyositis, polymyositis, and myositis [58–63]. IL-1 β induces accumulation of β -amyloid in skeletal muscle [62]. NLRP3 inflammasome promotes caspase activation, resulting in processing of IL-1 β and cell death, in response to cellular stresses [64–66]. It is likely that muscle wasting occurs by elevated levels of inflammatory IL-1 β in VCP muscle, particularly if such a high level is maintained for prolonged periods.

Inflammasomes are cytosolic multiprotein signaling pathways of innate immune system that sense pathogens and injury [4, 67–71]. Formation of an inflammasome involves dramatic re-localization of the inflammasome adapter protein apoptosis-associated speck-like protein containing a caspase recruitment domain (ASC) into a single speck [66]. Four major types of inflammasomes have been identified and defined by the NLR protein that they contain: (1) the NLRP1/NALP1b inflammasome [72, 73]; (2) the NLRC4/IPAF inflammasome [74–78]; (3) the NLRP3/NALP3 inflammasome [69, 79]; and (4) the AIM2 (absent in melanoma 2) containing inflammasome [80, 81]. The NLRP3/NALP3 inflammasome is activated by many

and diverse stimuli making it the most versatile and most clinically implicated inflammasome [70, 71, 82]. The NLRP3 inflammasome has been implicated in the pathogenesis of several neurodegenerative diseases, including Alzheimer's disease (AD), multiple sclerosis (MS), Parkinson's and traumatic brain injuries. Studies in AD have provided evidence that NLRP3 has an exacerbating role in the pathogenesis by showing data of NLRP3 and ASC association in amyloid-Beta stimulated glial cultures [83, 84]. Clinical studies in multiple sclerosis (MS) patients and brain trauma injury patients have suggested elevated levels of Caspase 1 (cleaved p10 and p20), pro-inflammatory IL-1 β , and IL-18 may be associated with the progression and pathology of the disease [85–87]. Similarly, studies in MS animal models have illustrated the presence of inflammasome-associated proteins such as ASC, Caspase 1 (cleaved p10 and p20), IL-1 β and IL-18, which may ultimately play a critical role in the pathogenesis of MS [88].

MCC950 has shown promising results in a study by *Coll et al.* (2015) illustrating attenuation of autoimmune encephalomyelitis (EAE) *in vivo* as well as rescue of neonatal lethality in a mouse model of CAPS [33]. MCC950 has also shown promise in autoinflammatory and autoimmune diseases. In this report, we did not detect activation of the NLRP3 inflammasome in the VCP mice brains of VCP-associated myopathy. However, not only did we discover a significant reduction in NLRP3 inflammasome and its mediators such as IL-1 β and IL-18 in the muscle and bones, but also found that the MCC950 inhibitor, significantly decreased activation of NLRP3 inflammasome associated „classic markers of VCP pathology“ (i.e. TDP-43 and p62/*SQSTM1*). The effects of MCC950 in our VCP iPSC-derived and murine myoblasts were highly significant in blocking the increase of NLRP3 inflammasome and its mediators IL-1 β , IL-18 and Caspase 1 (cleaved p10 and p20). These findings provide novel mechanistic insights into the activation of NLRP3 inflammasome pathways, which may possibly lead to therapeutic targets for treating NLRP3-associated VCP disease and related neuromuscular and neurodegenerative diseases. Discovering novel cellular and molecular anti-inflammatory targets will help ameliorate, not only VCP-associated myopathy, but also other common disorders such as ALS, sporadic inclusion body myositis, and other muscle diseases.

In summary, we report for the first time that the NLRP3 inflammasome pathway is highly activated in myoblasts derived from VCP patients and in the quadriceps muscles of VCP^{R155H/+} heterozygote mice. Both the muscle and the bone of VCP^{R155H/+} heterozygote mice displayed increased number of active macrophages producing iNOS and IL-1 β inflammatory mediators, which positively correlated with the severity of muscle wasting. Suppression of NLRP3 inflammasome activation, following treatment with MCC950 pharmacologic inhibitor, led to a significant amelioration of muscle strength in VCP^{R155H/+} heterozygote experimental mouse model of VCP-associated myopathy. Together, these results suggest that: (i) the NLRP3 inflammasome and local IL-1 β ⁽⁺⁾F4/80⁽⁺⁾Ly6C⁽⁺⁾ macrophages as novel players in the pathogenesis of VCP-associated myopathy; and (ii) identified the sulfonylurea MCC950 inhibitor of the NLRP3 inflammasome with promising therapeutic potential for the future treatment of patients with VCP-associated myopathy. While activation of NLRP3 inflammasome is associated with VCP-myopathy, whether and how this contributes to pathogenesis of VCP-myopathy remains to be determined.

Acknowledgments

The authors would like to thank the patients for providing muscle biopsies used in this study, Dr. John R. Lukens, Department of Immunology, St Jude Children's Research Hospital, Memphis, Tennessee 38105, USA and Vivien I Maltez, University of North Carolina at Chapel Hill, Department of Microbiology and Immunology for help with inflammasome experiments and critical discussion.

References

1. Bauernfeind F, Ablasser A, Bartok E, Kim S, Schmid-Burgk J, Cavlar T, Hornung V. Inflammasomes: current understanding and open questions. *Cell Mol Life Sci*. 2011; 68:765–783. [PubMed: 21072676]
2. Cassel SL, Joly S, Sutterwala FS. The NLRP3 inflammasome: a sensor of immune danger signals. *Semin Immunol*. 2009; 21:194–198. [PubMed: 19501527]
3. Cook GP, Savic S, Wittmann M, McDermott MF. The NLRP3 inflammasome, a target for therapy in diverse disease states. *Eur J Immunol*. 2010; 40:631–634. [PubMed: 20201018]
4. Schroder K, Zhou R, Tschopp J. The NLRP3 inflammasome: a sensor for metabolic danger? *Science*. 2010; 327:296–300. [PubMed: 20075245]
5. Strowig T, Henao-Mejia J, Elinav E, Flavell R. Inflammasomes in health and disease. *Nature*. 2012; 481:278–286. [PubMed: 22258606]
6. Heneka MT, Kummer MP, Latz E. Innate immune activation in neurodegenerative disease. *Nat Rev Immunol*. 2014; 14:463–477. [PubMed: 24962261]
7. Saresella M, Piancone F, Marventano I, Zoppis M, Hernis A, Zanette M, Trabattoni D, Chiappedi M, Ghezzi A, Canevini MP, et al. Multiple inflammasome complexes are activated in autistic spectrum disorders. *Brain Behav Immun*. 2016
8. Taga M, Minett T, Classey J, Matthews FE, Brayne C, Ince PG, Nicoll JA, Hugon J, Boche D, Mrc C. Metaflammasome components in the human brain: a role in dementia with Alzheimer's pathology? *Brain Pathol*. 2016
9. Couturier J, Stancu IC, Schakman O, Pierrot N, Huaux F, Kienlen-Campard P, Dewachter I, Octave JN. Activation of phagocytic activity in astrocytes by reduced expression of the inflammasome component ASC and its implication in a mouse model of Alzheimer disease. *J Neuroinflammation*. 2016; 13:20. [PubMed: 26818951]
10. Freeman LC, Ting JP. The pathogenic role of the inflammasome in neurodegenerative diseases. *J Neurochem*. 2016; 136(Suppl 1):29–38. [PubMed: 26119245]
11. Schmid-Burgk JL, Chauhan D, Schmidt T, Ebert TS, Reinhardt J, Endl E, Hornung V. A Genome-wide CRISPR (Clustered Regularly Interspaced Short Palindromic Repeats) Screen Identifies NEK7 as an Essential Component of NLRP3 Inflammasome Activation. *J Biol Chem*. 2016; 291:103–109. [PubMed: 26553871]
12. Olsen I, Singhrao SK. Inflammasome Involvement in Alzheimer's Disease. *J Alzheimers Dis*. 2016; 54:45–53. [PubMed: 27314526]
13. Kimonis VE, Fulchiero E, Vesa J, Watts G. VCP disease associated with myopathy, Paget disease of bone and frontotemporal dementia: review of a unique disorder. *Biochim Biophys Acta*. 2008; 1782:744–748. [PubMed: 18845250]
14. Kimonis VE, Mehta SG, Fulchiero EC, Thomasova D, Pasquali M, Boycott K, Neilan EG, Kartashov A, Forman MS, Tucker S, et al. Clinical studies in familial VCP myopathy associated with Paget disease of bone and frontotemporal dementia. *Am J Med Genet A*. 2008; 146A:745–757. [PubMed: 18260132]
15. Neumann M, Mackenzie IR, Cairns NJ, Boyer PJ, Markesbery WR, Smith CD, Taylor JP, Kretschmar HA, Kimonis VE, Forman MS. TDP-43 in the ubiquitin pathology of frontotemporal dementia with VCP gene mutations. *J Neuropathol Exp Neurol*. 2007; 66:152–157. [PubMed: 17279000]
16. Watts GD, Thomasova D, Ramdeen SK, Fulchiero EC, Mehta SG, Drachman DA, Weihl CC, Jamrozik Z, Kwiecinski H, Kaminska A, Kimonis VE. Novel VCP mutations in inclusion body

- myopathy associated with Paget disease of bone and frontotemporal dementia. *Clin Genet.* 2007; 72:420–426. [PubMed: 17935506]
17. Kimonis VE, Kovach MJ, Waggoner B, Leal S, Salam A, Rimer L, Davis K, Khardori R, Gelber D. Clinical and molecular studies in a unique family with autosomal dominant limb-girdle muscular dystrophy and Paget disease of bone. *Genet Med.* 2000; 2:232–241. [PubMed: 11252708]
 18. Dec E, Rana P, Katheria V, Dec R, Khare M, Nalbandian A, Leu SY, Radom-Aizik S, Llewellyn K, BenMohamed L, et al. Cytokine profiling in patients with VCP-associated disease. *Clin Transl Sci.* 2014; 7:29–32. [PubMed: 24119107]
 19. Roca I, Requena J, Edel MJ, Alvarez-Palomo AB. Myogenic Precursors from iPSC Cells for Skeletal Muscle Cell Replacement Therapy. *J Clin Med.* 2015; 4:243–259. [PubMed: 26239126]
 20. Salani S, Donadoni C, Rizzo F, Bresolin N, Comi GP, Corti S. Generation of skeletal muscle cells from embryonic and induced pluripotent stem cells as an in vitro model and for therapy of muscular dystrophies. *J Cell Mol Med.* 2012; 16:1353–1364. [PubMed: 22129481]
 21. Llewellyn KJ, Nalbandian A, Jung KM, Nguyen C, Avanesian A, Mozaffar T, Piomelli D, Kimonis VE. Lipid-enriched diet rescues lethality and slows down progression in a murine model of VCP-associated disease. *Hum Mol Genet.* 2014; 23:1333–1344. [PubMed: 24158850]
 22. Deacon RM. Measuring the strength of mice. *J Vis Exp.* 2013
 23. Capers PL, Hyacinth HI, Cue S, Chappa P, Vikulina T, Roser-Page S, Weitzmann MN, Archer DR, Newman GW, Quarshie A, et al. Body composition and grip strength are improved in transgenic sickle mice fed a high-protein diet. *J Nutr Sci.* 2015; 4:e6. [PubMed: 26090102]
 24. Nevins ME, Nash SA, Beardsley PM. Quantitative grip strength assessment as a means of evaluating muscle relaxation in mice. *Psychopharmacology (Berl).* 1993; 110:92–96. [PubMed: 7870904]
 25. Wolf E, Wanke R, Schenck E, Hermanns W, Brem G. Effects of growth hormone overproduction on grip strength of transgenic mice. *Eur J Endocrinol.* 1995; 133:735–740. [PubMed: 8548060]
 26. Nalbandian A, Llewellyn KJ, Badadani M, Yin HZ, Nguyen C, Katheria V, Watts G, Mukherjee J, Vesa J, Caiozzo V, et al. A progressive translational mouse model of human valosin-containing protein disease: the VCP(R155H/+) mouse. *Muscle Nerve.* 2013; 47:260–270. [PubMed: 23169451]
 27. Nalbandian A, Nguyen C, Katheria V, Llewellyn KJ, Badadani M, Caiozzo V, Kimonis VE. Exercise training reverses skeletal muscle atrophy in an experimental model of VCP disease. *PLoS One.* 2013; 8:e76187. [PubMed: 24130765]
 28. Zhang X, Chentoufi AA, Dasgupta G, Nesburn AB, Wu M, Zhu X, Carpenter D, Wechsler SL, You S, BenMohamed L. A genital tract peptide epitope vaccine targeting TLR-2 efficiently induces local and systemic CD8+ T cells and protects against herpes simplex virus type 2 challenge. *Mucosal Immunol.* 2009; 2:129–143. [PubMed: 19129756]
 29. Uchida A, Sasaguri H, Kimura N, Tajiri M, Ohkubo T, Ono F, Sakaue F, Kanai K, Hirai T, Sano T, et al. Non-human primate model of amyotrophic lateral sclerosis with cytoplasmic mislocalization of TDP-43. *Brain.* 2012; 135:833–846. [PubMed: 22252998]
 30. Xu Z, Yang C. TDP-43-The key to understanding amyotrophic lateral sclerosis. *Rare Dis.* 2014; 2:e944443. [PubMed: 26942097]
 31. Wils H, Kleinberger G, Janssens J, Pereson S, Joris G, Cuijt I, Smits V, Ceuterick-de Groote C, Van Broeckhoven C, Kumar-Singh S. TDP-43 transgenic mice develop spastic paralysis and neuronal inclusions characteristic of ALS and frontotemporal lobar degeneration. *Proc Natl Acad Sci U S A.* 2010; 107:3858–3863. [PubMed: 20133711]
 32. Geser F, Prvulovic D, O'Dwyer L, Hardiman O, Bede P, Bokde AL, Trojanowski JQ, Hampel H. On the development of markers for pathological TDP-43 in amyotrophic lateral sclerosis with and without dementia. *Prog Neurobiol.* 2011; 95:649–662. [PubMed: 21911035]
 33. Coll RC, Robertson AA, Chae JJ, Higgins SC, Munoz-Planillo R, Inserra MC, Vetter I, Dungan LS, Monks BG, Stutz A, et al. A small-molecule inhibitor of the NLRP3 inflammasome for the treatment of inflammatory diseases. *Nat Med.* 2015; 21:248–255. [PubMed: 25686105]
 34. Nalbandian A, Llewellyn KJ, Kitazawa M, Yin HZ, Badadani M, Khanlou N, Edwards R, Nguyen C, Mukherjee J, Mozaffar T, et al. The homozygote VCP(R(1)(5)(5)H/R(1)(5)(5)H) mouse model

- exhibits accelerated human VCP-associated disease pathology. *PLoS One*. 2012; 7:e46308. [PubMed: 23029473]
35. Badadani M, Nalbandian A, Watts GD, Vesa J, Kitazawa M, Su H, Tanaja J, Dec E, Wallace DC, Mukherjee J, et al. VCP associated inclusion body myopathy and paget disease of bone knock-in mouse model exhibits tissue pathology typical of human disease. *PLoS One*. 2010; 5
 36. Gross CJ, Gross O. The Nlrp3 inflammasome admits defeat. *Trends Immunol*. 2015; 36:323–324. [PubMed: 25991463]
 37. Dalakas MC. Mechanistic effects of IVIg in neuroinflammatory diseases: conclusions based on clinicopathologic correlations. *J Clin Immunol*. 2014; 34(Suppl 1):S120–126. [PubMed: 24722854]
 38. Grunblatt E, Mandel S, Youdim MB. Neuroprotective strategies in Parkinson's disease using the models of 6-hydroxydopamine and MPTP. *Ann N Y Acad Sci*. 2000; 899:262–273. [PubMed: 10863545]
 39. Tuon T, Souza PS, Santos MF, Pereira FT, Pedroso GS, Luciano TF, De Souza CT, Dutra RC, Silveira PC, Pinho RA. Physical Training Regulates Mitochondrial Parameters and Neuroinflammatory Mechanisms in an Experimental Model of Parkinson's Disease. *Oxid Med Cell Longev*. 2015; 2015:261809. [PubMed: 26448816]
 40. Kovach MJ, Waggoner B, Leal SM, Gelber D, Khardori R, Levenstien MA, Shanks CA, Gregg G, Al-Lozi MT, Miller T, et al. Clinical delineation and localization to chromosome 9p13.3-p12 of a unique dominant disorder in four families: hereditary inclusion body myopathy, Paget disease of bone, and frontotemporal dementia. *Mol Genet Metab*. 2001; 74:458–475. [PubMed: 11749051]
 41. Watts GD, Wymer J, Kovach MJ, Mehta SG, Mumm S, Darvish D, Pestronk A, Whyte MP, Kimonis VE. Inclusion body myopathy associated with Paget disease of bone and frontotemporal dementia is caused by mutant valosin-containing protein. *Nat Genet*. 2004; 36:377–381. [PubMed: 15034582]
 42. Joassard OR, Amirouche A, Gallot YS, Desgeorges MM, Castells J, Durieux AC, Berthon P, Freyssenet DG. Regulation of Akt-mTOR, ubiquitin-proteasome and autophagy-lysosome pathways in response to formoterol administration in rat skeletal muscle. *Int J Biochem Cell Biol*. 2013; 45:2444–2455. [PubMed: 23916784]
 43. Tamura Y, Kitaoka Y, Matsunaga Y, Hoshino D, Hatta H. Daily heat stress treatment rescues denervation-activated mitochondrial clearance and atrophy in skeletal muscle. *J Physiol*. 2015; 593:2707–2720. [PubMed: 25900738]
 44. Nalbandian A, Llewellyn KJ, Nguyen C, Yazdi PG, Kimonis VE. Rapamycin and chloroquine: the in vitro and in vivo effects of autophagy-modifying drugs show promising results in valosin containing protein multisystem proteinopathy. *PLoS One*. 2015; 10:e0122888. [PubMed: 25884947]
 45. Shen YF, Tang Y, Zhang XJ, Huang KX, Le WD. Adaptive changes in autophagy after UPS impairment in Parkinson's disease. *Acta Pharmacol Sin*. 2013; 34:667–673. [PubMed: 23503475]
 46. Halle A, Hornung V, Petzold GC, Stewart CR, Monks BG, Reinheckel T, Fitzgerald KA, Latz E, Moore KJ, Golenbock DT. The NALP3 inflammasome is involved in the innate immune response to amyloid-beta. *Nat Immunol*. 2008; 9:857–865. [PubMed: 18604209]
 47. Heneka MT, Kummer MP, Stutz A, Delekate A, Schwartz S, Vieira-Saecker A, Griep A, Axt D, Remus A, Tzeng TC, et al. NLRP3 is activated in Alzheimer's disease and contributes to pathology in APP/PS1 mice. *Nature*. 2013; 493:674–678. [PubMed: 23254930]
 48. Singhal G, Jaehne EJ, Corrigan F, Toben C, Baune BT. Inflammasomes in neuroinflammation and changes in brain function: a focused review. *Front Neurosci*. 2014; 8:315. [PubMed: 25339862]
 49. Tan MS, Yu JT, Jiang T, Zhu XC, Tan L. The NLRP3 inflammasome in Alzheimer's disease. *Mol Neurobiol*. 2013; 48:875–882. [PubMed: 23686772]
 50. Tan MS, Yu JT, Jiang T, Zhu XC, Wang HF, Zhang W, Wang YL, Jiang W, Tan L. NLRP3 polymorphisms are associated with late-onset Alzheimer's disease in Han Chinese. *J Neuroimmunol*. 2013; 265:91–95. [PubMed: 24144834]
 51. Fink SL, Cookson BT. Apoptosis, pyroptosis, and necrosis: mechanistic description of dead and dying eukaryotic cells. *Infect Immun*. 2005; 73:1907–1916. [PubMed: 15784530]

52. Mariathasan S, Newton K, Monack DM, Vucic D, French DM, Lee WP, Roose-Girma M, Erickson S, Dixit VM. Differential activation of the inflammasome by caspase-1 adaptors ASC and Ipaf. *Nature*. 2004; 430:213–218. [PubMed: 15190255]
53. Heneka MT, Carson MJ, El Khoury J, Landreth GE, Brosseron F, Feinstein DL, Jacobs AH, Wyss-Coray T, Vitorica J, Ransohoff RM, et al. Neuroinflammation in Alzheimer's disease. *Lancet Neurol*. 2015; 14:388–405. [PubMed: 25792098]
54. Broderick L, De Nardo D, Franklin BS, Hoffman HM, Latz E. The inflammasomes and autoinflammatory syndromes. *Annu Rev Pathol*. 2015; 10:395–424. [PubMed: 25423351]
55. De Nardo D, Latz E. NLRP3 inflammasomes link inflammation and metabolic disease. *Trends Immunol*. 2011; 32:373–379. [PubMed: 21733753]
56. Shao BZ, Xu ZQ, Han BZ, Su DF, Liu C. NLRP3 inflammasome and its inhibitors: a review. *Front Pharmacol*. 2015; 6:262. [PubMed: 26594174]
57. Rawat R, Cohen TV, Ampong B, Francia D, Henriques-Pons A, Hoffman EP, Nagaraju K. Inflammasome up-regulation and activation in dysferlin-deficient skeletal muscle. *Am J Pathol*. 2010; 176:2891–2900. [PubMed: 20413686]
58. Lundberg I, Kratz AK, Alexanderson H, Patarroyo M. Decreased expression of interleukin-1alpha, interleukin-1beta, and cell adhesion molecules in muscle tissue following corticosteroid treatment in patients with polymyositis and dermatomyositis. *Arthritis Rheum*. 2000; 43:336–348. [PubMed: 10693873]
59. Tucci M, Quatraro C, Dammacco F, Silvestris F. Interleukin-18 overexpression as a hallmark of the activity of autoimmune inflammatory myopathies. *Clin Exp Immunol*. 2006; 146:21–31. [PubMed: 16968394]
60. Tucci M, Quatraro C, Dammacco F, Silvestris F. Increased IL-18 production by dendritic cells in active inflammatory myopathies. *Ann N Y Acad Sci*. 2007; 1107:184–192. [PubMed: 17804546]
61. Lunemann JD, Schmidt J, Schmid D, Barthel K, Wrede A, Dalakas MC, Munz C. Beta-amyloid is a substrate of autophagy in sporadic inclusion body myositis. *Ann Neurol*. 2007; 61:476–483. [PubMed: 17469125]
62. Schmidt J, Barthel K, Wrede A, Salajegheh M, Bahr M, Dalakas MC. Interrelation of inflammation and APP in sIBM: IL-1 beta induces accumulation of beta-amyloid in skeletal muscle. *Brain*. 2008; 131:1228–1240. [PubMed: 18420712]
63. Schmidt J, Barthel K, Zschuntzsch J, Muth IE, Swindle EJ, Hombach A, Sehmisch S, Wrede A, Luhder F, Gold R, Dalakas MC. Nitric oxide stress in sporadic inclusion body myositis muscle fibres: inhibition of inducible nitric oxide synthase prevents interleukin-1beta-induced accumulation of beta-amyloid and cell death. *Brain*. 2012; 135:1102–1114. [PubMed: 22436237]
64. Schaale K, Peters KM, Murthy AM, Fritzsche AK, Phan MD, Totsika M, Robertson AA, Nichols KB, Cooper MA, Stacey KJ, et al. Strain- and host species-specific inflammasome activation, IL-1beta release, and cell death in macrophages infected with uropathogenic *Escherichia coli*. *Mucosal Immunol*. 2015
65. Sester DP, Sagulenko V, Thygesen SJ, Cridland JA, Loi YS, Cridland SO, Masters SL, Genske U, Hornung V, Andoniou CE, et al. Deficient NLRP3 and AIM2 Inflammasome Function in Autoimmune NZB Mice. *J Immunol*. 2015; 195:1233–1241. [PubMed: 26116505]
66. Sester DP, Thygesen SJ, Sagulenko V, Vajjhala PR, Cridland JA, Vitak N, Chen KW, Osborne GW, Schroder K, Stacey KJ. A novel flow cytometric method to assess inflammasome formation. *J Immunol*. 2015; 194:455–462. [PubMed: 25404358]
67. Schroder K, Tschopp J. The inflammasomes. *Cell*. 2010; 140:821–832. [PubMed: 20303873]
68. Tschopp J, Schroder K. NLRP3 inflammasome activation: The convergence of multiple signalling pathways on ROS production? *Nat Rev Immunol*. 2010; 10:210–215. [PubMed: 20168318]
69. Abderrazak A, Syrovets T, Couchie D, El Hadri K, Friguet B, Simmet T, Rouis M. NLRP3 inflammasome: From a danger signal sensor to a regulatory node of oxidative stress and inflammatory diseases. *Redox Biol*. 2015; 4C:296–307.
70. Rathinam VA, Vanaja SK, Waggoner L, Sokolovska A, Becker C, Stuart LM, Leong JM, Fitzgerald KA. TRIF licenses caspase-11-dependent NLRP3 inflammasome activation by gram-negative bacteria. *Cell*. 2012; 150:606–619. [PubMed: 22819539]

71. Vanaja SK, Rathinam VA, Fitzgerald KA. Mechanisms of inflammasome activation: recent advances and novel insights. *Trends Cell Biol.* 2015
72. Boyden ED, Dietrich WF. Nalp1b controls mouse macrophage susceptibility to anthrax lethal toxin. *Nat Genet.* 2006; 38:240–244. [PubMed: 16429160]
73. Mawhinney LJ, de Rivero Vaccari JP, Dale GA, Keane RW, Bramlett HM. Heightened inflammasome activation is linked to age-related cognitive impairment in Fischer 344 rats. *BMC Neurosci.* 2011; 12:123. [PubMed: 22133203]
74. Zhao Y, Yang J, Shi J, Gong YN, Lu Q, Xu H, Liu L, Shao F. The NLRC4 inflammasome receptors for bacterial flagellin and type III secretion apparatus. *Nature.* 2011; 477:596–600. [PubMed: 21918512]
75. Miao EA, Alpuche-Aranda CM, Dors M, Clark AE, Bader MW, Miller SI, Aderem A. Cytoplasmic flagellin activates caspase-1 and secretion of interleukin 1beta via Ipaf. *Nat Immunol.* 2006; 7:569–575. [PubMed: 16648853]
76. Miao EA, Mao DP, Yudkovsky N, Bonneau R, Lorang CG, Warren SE, Leaf IA, Aderem A. Innate immune detection of the type III secretion apparatus through the NLRC4 inflammasome. *Proc Natl Acad Sci U S A.* 2010; 107:3076–3080. [PubMed: 20133635]
77. Silveira TN, Zamboni DS. Pore formation triggered by *Legionella* spp. is an Nlr4 inflammasome-dependent host cell response that precedes pyroptosis. *Infect Immun.* 2010; 78:1403–1413. [PubMed: 20048047]
78. Akhter A, Gavrilin MA, Frantz L, Washington S, Ditty C, Limoli D, Day C, Sarkar A, Newland C, Butchar J, et al. Caspase-7 activation by the Nlr4/Ipaf inflammasome restricts *Legionella pneumophila* infection. *PLoS Pathog.* 2009; 5:e1000361. [PubMed: 19343209]
79. Martinon F, Petrilli V, Mayor A, Tardivel A, Tschopp J. Gout-associated uric acid crystals activate the NALP3 inflammasome. *Nature.* 2006; 440:237–241. [PubMed: 16407889]
80. Hornung V, Ablasser A, Charrel-Dennis M, Bauernfeind F, Horvath G, Caffrey DR, Latz E, Fitzgerald KA. AIM2 recognizes cytosolic dsDNA and forms a caspase-1-activating inflammasome with ASC. *Nature.* 2009; 458:514–518. [PubMed: 19158675]
81. Fernandes-Alnemri T, Yu JW, Datta P, Wu J, Alnemri ES. AIM2 activates the inflammasome and cell death in response to cytoplasmic DNA. *Nature.* 2009; 458:509–513. [PubMed: 19158676]
82. Sokolovska A, Becker CE, Ip WK, Rathinam VA, Brudner M, Paquette N, Tanne A, Vanaja SK, Moore KJ, Fitzgerald KA, et al. Activation of caspase-1 by the NLRP3 inflammasome regulates the NADPH oxidase NOX2 to control phagosome function. *Nat Immunol.* 2013; 14:543–553. [PubMed: 23644505]
83. Blum-Degen D, Frolich L, Hoyer S, Riederer P. Altered regulation of brain glucose metabolism as a cause of neurodegenerative disorders? *J Neural Transm Suppl.* 1995; 46:139–147. [PubMed: 8821049]
84. Blum-Degen D, Muller T, Kuhn W, Gerlach M, Przuntek H, Riederer P. Interleukin-1 beta and interleukin-6 are elevated in the cerebrospinal fluid of Alzheimer's and de novo Parkinson's disease patients. *Neurosci Lett.* 1995; 202:17–20. [PubMed: 8787820]
85. Franchi L, Amer A, Body-Malapel M, Kanneganti TD, Ozoren N, Jagirdar R, Inohara N, Vandenabeele P, Bertin J, Coyle A, et al. Cytosolic flagellin requires Ipaf for activation of caspase-1 and interleukin 1beta in salmonella-infected macrophages. *Nat Immunol.* 2006; 7:576–582. [PubMed: 16648852]
86. Kummer JA, Broekhuizen R, Everett H, Agostini L, Kuijk L, Martinon F, van Bruggen R, Tschopp J. Inflammasome components NALP 1 and 3 show distinct but separate expression profiles in human tissues suggesting a site-specific role in the inflammatory response. *J Histochem Cytochem.* 2007; 55:443–452. [PubMed: 17164409]
87. Martinon F, Tschopp J. Inflammatory caspases and inflammasomes: master switches of inflammation. *Cell Death Differ.* 2007; 14:10–22. [PubMed: 16977329]
88. Karni A, Koldzic DN, Bharanidharan P, Khoury SJ, Weiner HL. IL-18 is linked to raised IFN-gamma in multiple sclerosis and is induced by activated CD4(+) T cells via CD40-CD40 ligand interactions. *J Neuroimmunol.* 2002; 125:134–140. [PubMed: 11960649]

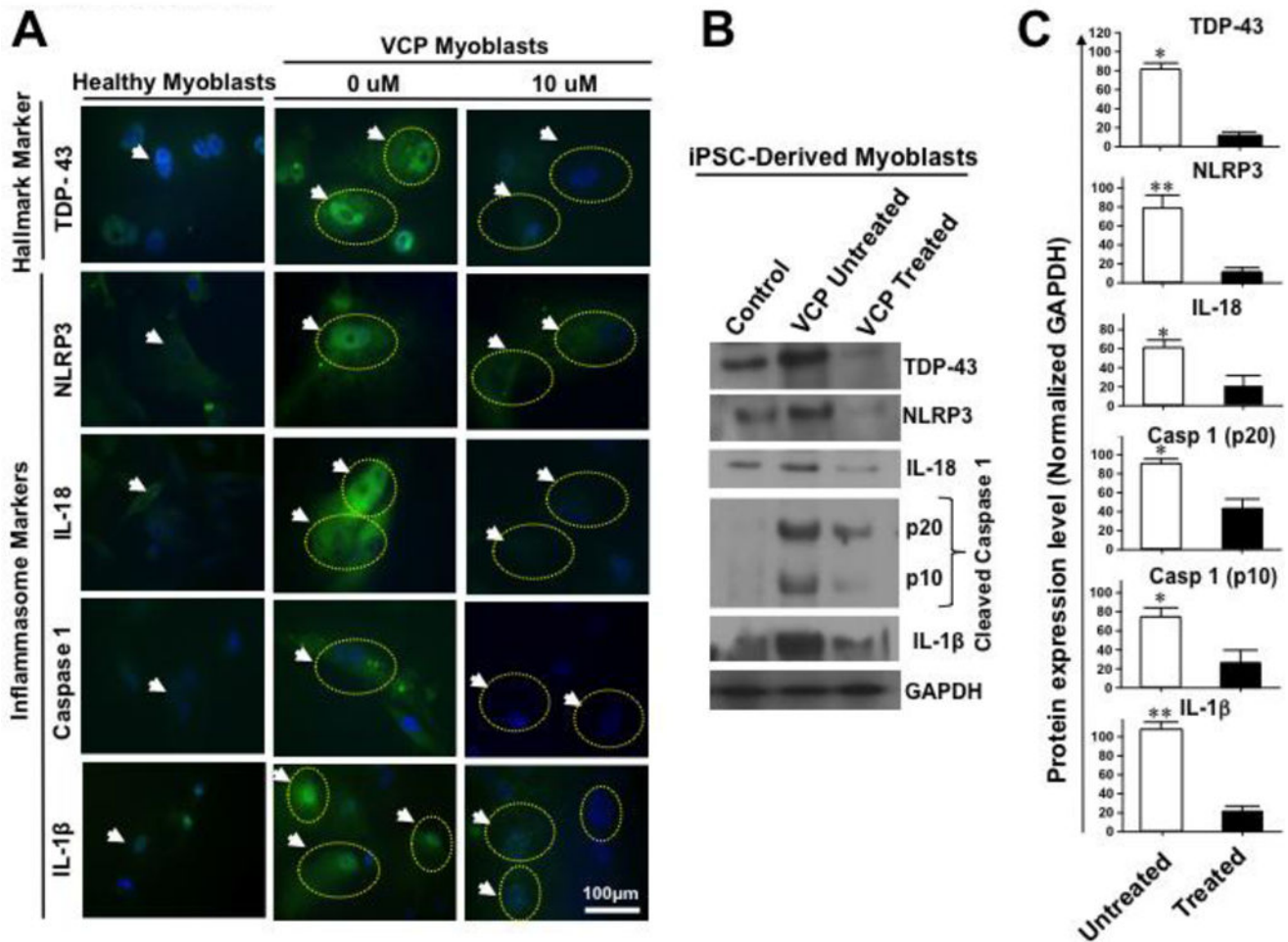


Figure 1. NLRP3 inflammasome pathway is active in myoblasts from VCP patients
(A) Immunohistochemical analysis of NLRP3 cascade mediators in iPSC-derived healthy myoblasts (*left panel*) and VCP disease myoblasts (*middle panel*, 0 μ M) were immunostained with mAbs specific to human TDP-43 ('classic' marker of VCP pathology), and NLRP3, IL-18, Caspase 1, and IL-1 β (markers of inflammasome activation) and then analyzed by confocal microscopy. White arrows and yellow dotted circles indicate to positive staining in VCP myoblasts. The *right panel*, 10 μ M shows VCP disease myoblasts treated with MCC950 inhibitor at 10 μ M and immunostained with TDP-43, NLRP3, IL-18, Caspase 1, and IL-1 β mAbs. White arrows and yellow dotted circles point to fading of positive staining in VCP myoblasts following MCC950 inhibitor treatment. DAPI (blue) indicates staining of nuclei, and FITC (green) indicates staining with the various inflammasome markers including NLRP3, IL-18, Caspase 1, and IL-1 β in myoblasts from VCP patients. **(B)** Western blot analysis of TDP-43, NLRP3, IL-18, Caspase 1, and IL-1 β proteins from iPSC-derived healthy myoblasts (*control*) and from VCP disease myoblasts either untreated (*VCP untreated*) or treated with 10 μ M of MCC950 inhibitor (*VCP treated*). GAPDH was used as a positive loading control. **(C)** Western blot results from three experiments normalized to GAPDH. Experiments shown are representative of independently performed triplicates. (*) Indicates $P < 0.05$ and (**) indicates $P < 0.01$ calculated by Mann-

Whitney test and two-tailed *t*-tests when comparing protein expression of each marker in treated vs. untreated human VCP myoblasts.

Author Manuscript

Author Manuscript

Author Manuscript

Author Manuscript

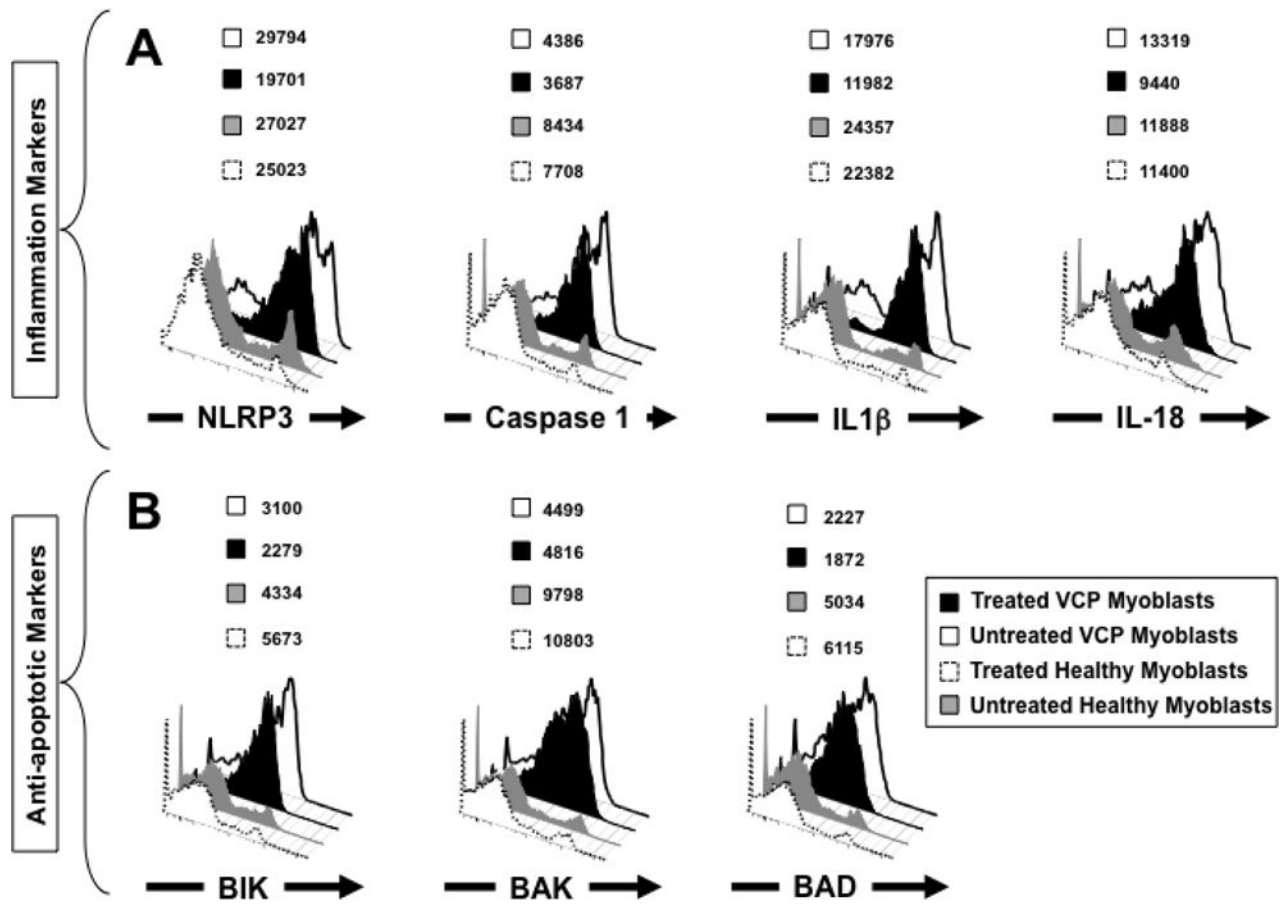


Figure 2. Level of expression of NLRP3 inflammasome activation markers in myoblasts from VCP patients

(A) FACS analysis of NLRP3 cascade mediators in iPSC-derived myoblasts from VCP patients that are either left untreated (*white*) or treated with the MCC950 specific inhibitor of NLRP3 inflammasome (*black*). Treated and untreated VCP myoblasts were stained with mAbs specific to human NLRP3, Caspase 1, IL-1 β and IL-18 (markers of inflammasome activation) and then analyzed by flow cytometry. iPSC-derived myoblasts from healthy patients that are either left untreated (*gray*) or treated with MCC950 specific inhibitor of NLRP3 inflammasome (*dotted line*) were used as negative controls. (B) FACS analysis of anti-apoptotic markers BIK, BAK, and BAD in iPSC-derived myoblasts from VCP patients and healthy controls. Experiments shown are representative of independently performed triplicates. (*) Indicates $P < 0.05$ and (**) indicates $P < 0.01$ calculated by Mann-Whitney test and two-tailed t -tests when comparing protein expression of each marker in treated vs. untreated human VCP myoblasts.

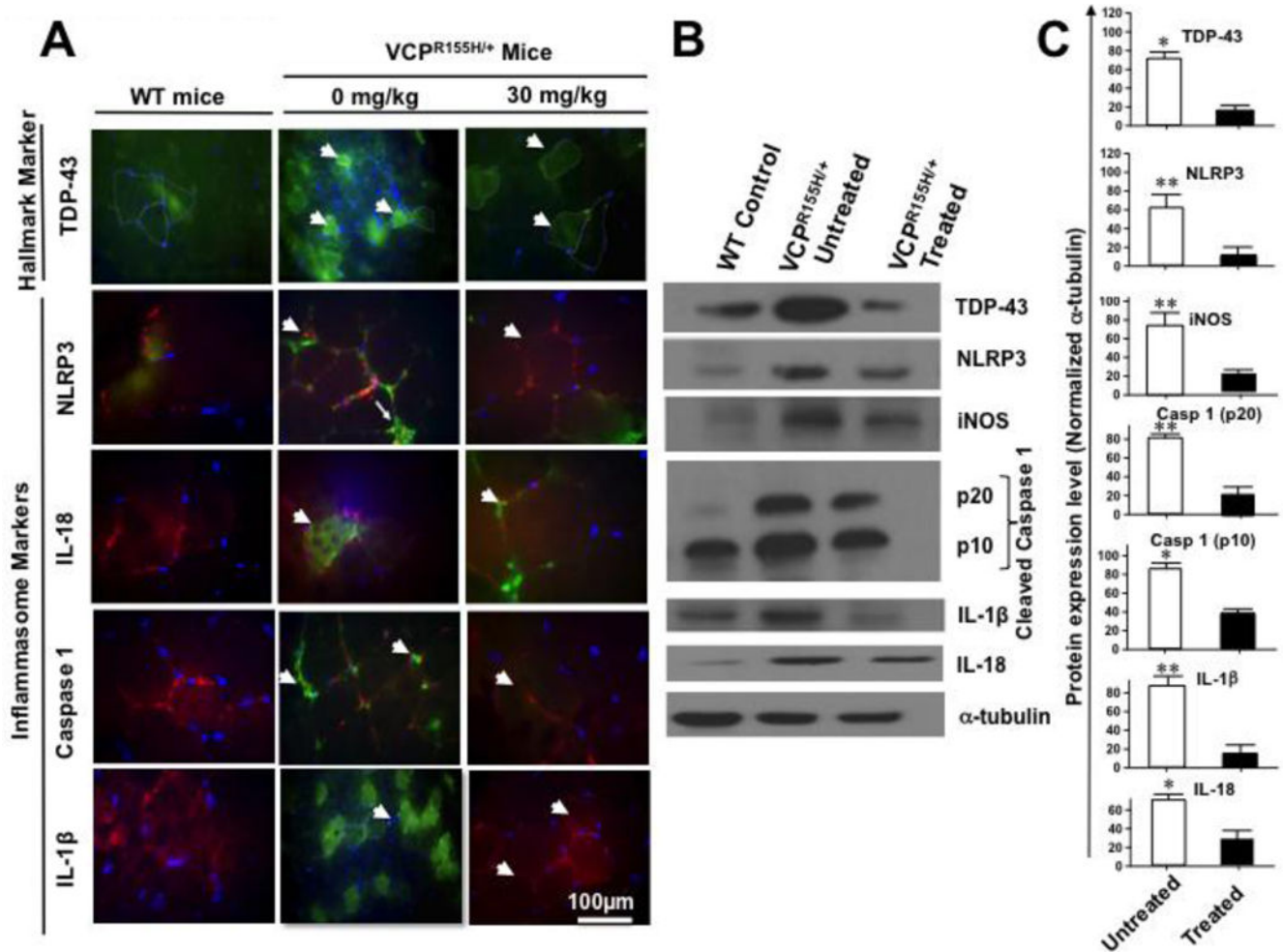


Figure 3. Expression of NLRP3 inflammasome and pathology markers in quadriceps femoris muscles of $VCP^{R155H/+}$ heterozygote mice

(A) Immunohistochemical analysis of NLRP3 cascade mediators in quadriceps muscles of $VCP^{R155H/+}$ heterozygote mice. Sections of quadriceps femoris muscles from control wild type mice ($n = 8$, left panel) and 2-year old $VCP^{R155H/+}$ heterozygote mice ($n = 8$, middle panel, $VCP^{R155H/+}$ 0-mg/kg) were immunostained with mAbs specific to mouse TDP-43 („classic“ marker of VCP pathology), and NLRP3, IL-18, Caspase 1, and IL-1 β (inflammasome markers) and then analyzed by fluorescence microscopy. White arrows indicate positive staining of myoblasts; TRITC (red, stained with laminin) identify muscle membrane of muscle fibers. DAPI (blue) indicates staining of nuclei. The right panel shows staining of section of quadriceps muscles from 2-year-old $VCP^{R155H/+}$ heterozygote mice treated with MCC950 inhibitor at 30 mg/kg ($VCP^{R155H/+}$, 30-mg/kg) and immunostained with TDP-43, NLRP3, IL-18, Caspase 1, and IL-1 β mAbs (FITC, green). White arrows point to decreased positive staining in mouse myoblasts following MCC950 inhibitor treatment. TRITC-stained (red, stained with laminin) identify muscle membrane of muscle fibers. DAPI (blue) indicates staining of nuclei. (B) Western blot analysis of TDP-43, NLRP3, iNOS, Caspase 1 (p20 and p10), IL-1 β , IL-18 and α -tubulin proteins from quadriceps muscles of wild type mice ($n = 8$, WT control) and from myoblasts from 2-year-

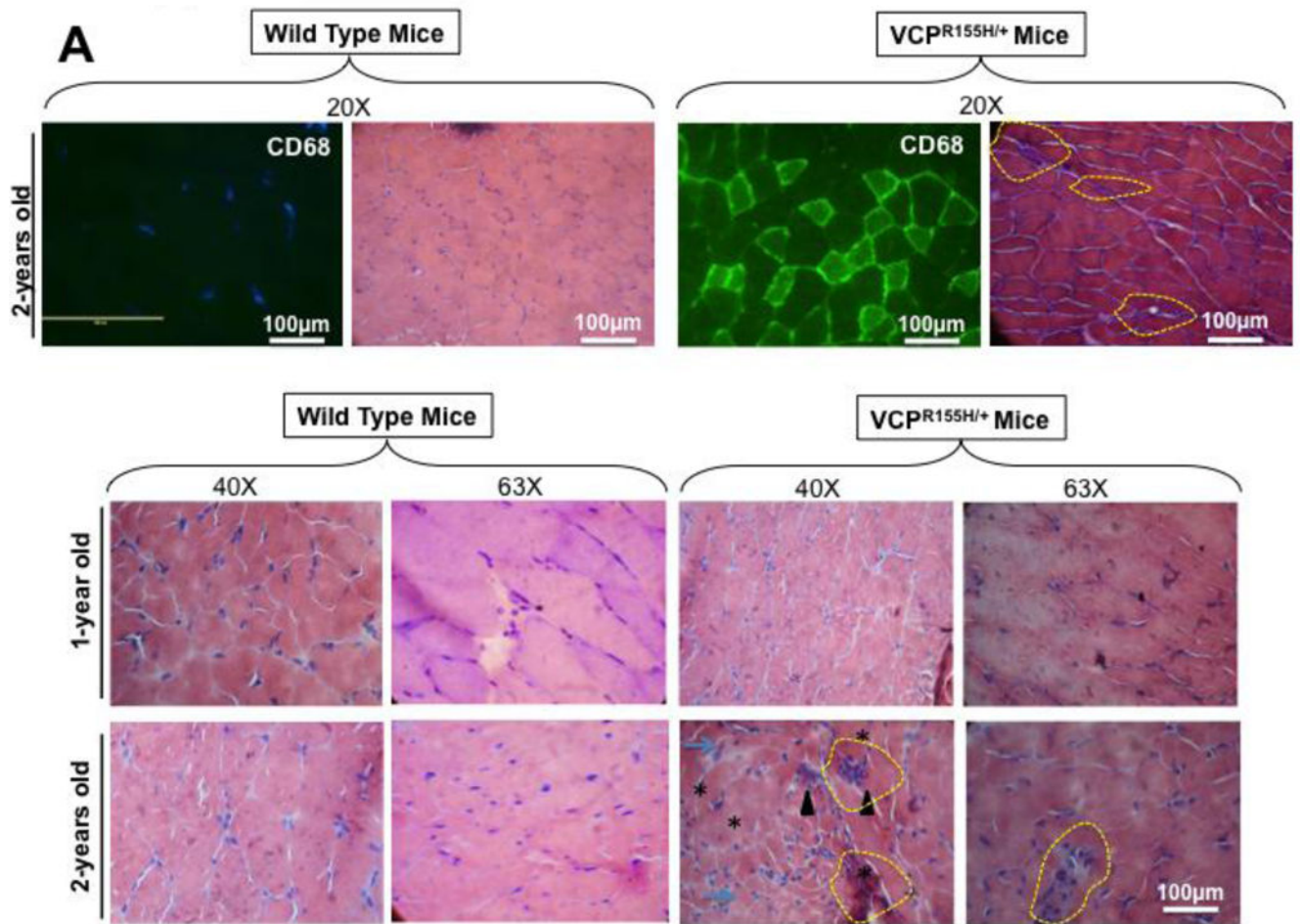
old $VCP^{R155H/+}$ heterozygote mice either left untreated ($n = 8$, $VCP^{R155H/+}$ untreated) or treated with 30-mg/kg of MCC950 inhibitor ($VCP^{R155H/+}$ Treated). (C) Western blot results from three experiments normalized to α -tubulin, positive loading control. Experiments shown are representative of independently performed triplicates. (*) Represents the $P < 0.05$ calculated by two-tailed and Mann-Whitney t -tests when comparing protein expression of each marker in quadriceps muscles of treated vs. untreated myoblasts from $VCP^{R155H/+}$ heterozygote mice.

Author Manuscript

Author Manuscript

Author Manuscript

Author Manuscript

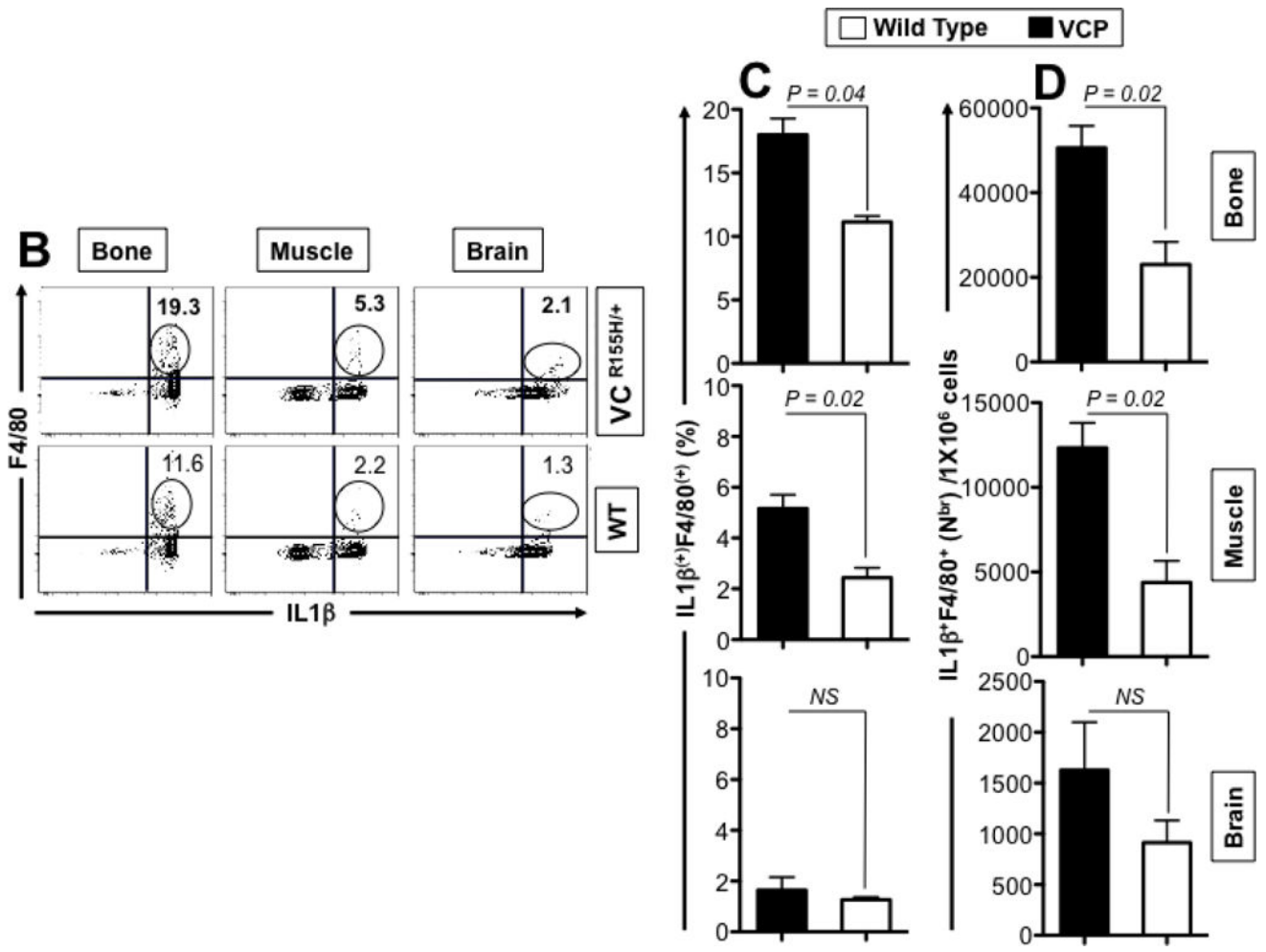


Author Manuscript

Author Manuscript

Author Manuscript

Author Manuscript



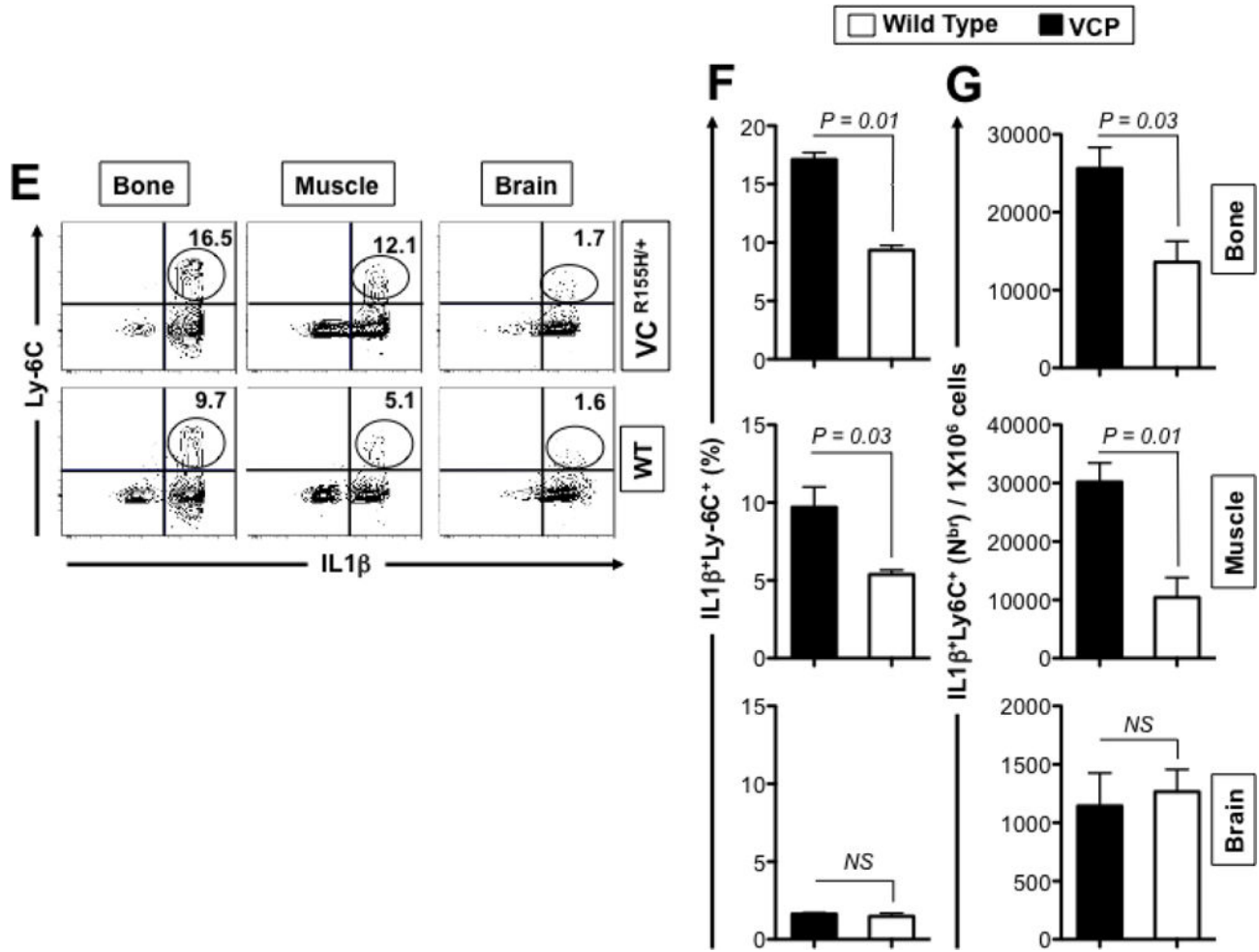
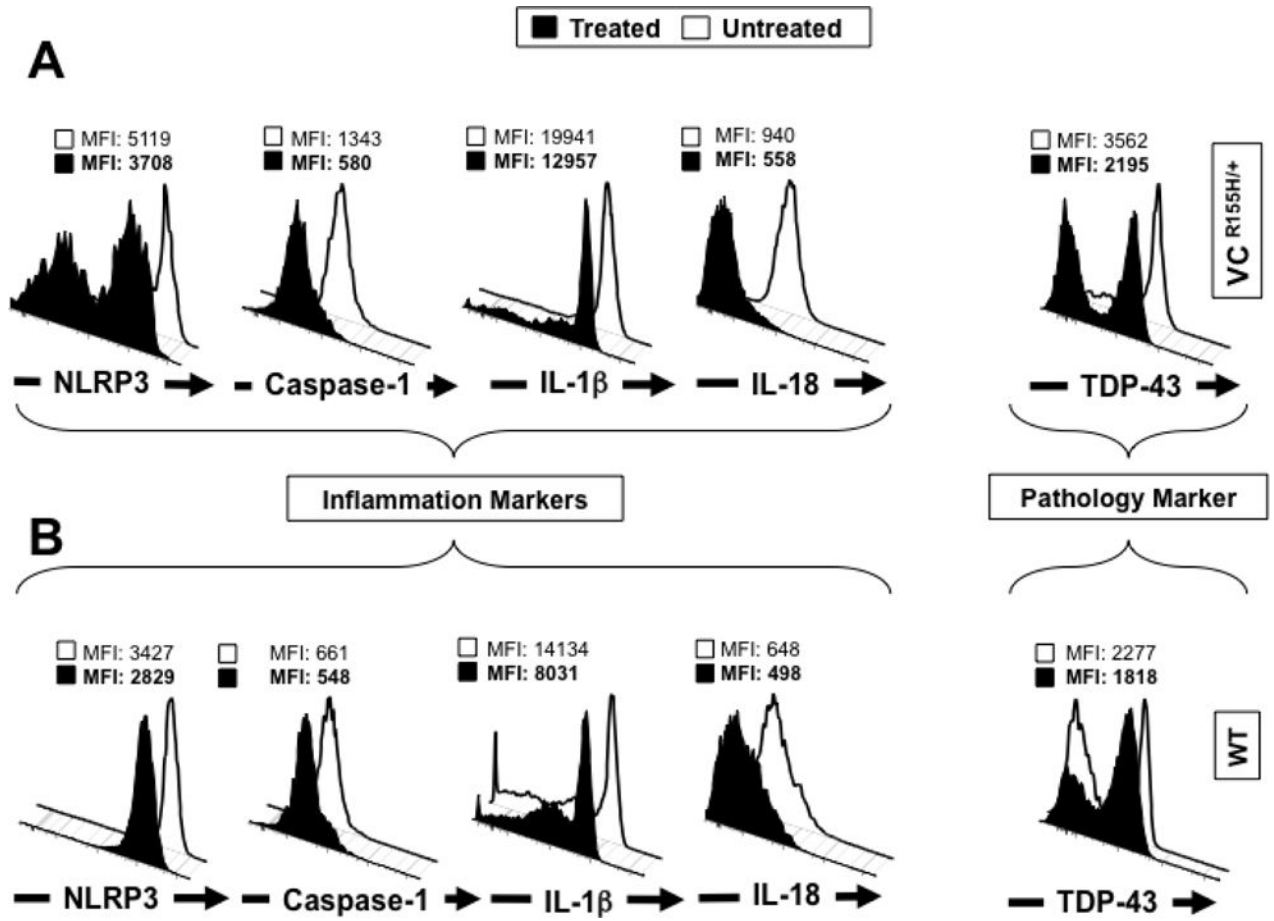


Figure 4. Histology and FACS analysis of *iNOS*- and *IL-1β*-producing inflammatory macrophages infiltrating bone, muscle and brain of *VCP^{R155H/+}* heterozygote mice

(A) Two-years-old *VCP^{R155H/+}* heterozygote and WT littermate mice were immunostained with CD68, a glycoprotein expressed on monocytes and macrophages (Magnification at 20×) and in parallel stained with Hematoxylin and eosin (Magnification at 20×). H&E sections show cell infiltrates in muscle of 1- and 2-years-old *VCP^{R155H/+}* heterozygote and WT littermate mice (Magnifications at 40× and 63×). As depicted, triangular black arrows show fibrosis, blue arrows depict central nucleation indicating regeneration, asterisks show degenerating fibers, and yellow arrows and yellow dotted lines point to persistent neutrophils, macrophages and necrotic myocytes. (B) Cell suspensions were harvested from bones, muscles and brains of 24-month old perfused *VCP^{R155H/+}* heterozygote mice ($n = 8$) and double stained using a mAb specific to mouse macrophages F4/80 surface marker (clone BM8) and a mAb specific to a mouse intracellular *IL-1β* (clone B122). Cell suspensions from bones, muscles and brains of 24-month old wild type mice ($n = 8$) used as controls were stained in parallel. Representative dot plot figure showing the percentages of $F4/80^{+}IL-1\beta^{+}$ macrophages determined in bones, muscles and brains from *VCP^{R155H/+}* heterozygote mice vs. WT mice. The bar graphs represent the means and SD of the percentages (C) and number (D) of $IL-1\beta^{+}F4/80^{+}$ macrophages in bones, muscles and

brains from a group of 8 VCP^{R155H/+} heterozygote mice and 8 WT mice. **(E)** Cell suspensions were harvested from bone, muscle and brain of 24-month old perfused VCP^{R155H/+} heterozygote mice and double stained using a mAb specific to Ly6C activation marker of mouse macrophages (clone 1A8) and a mAb specific to a mouse intracellular IL-1 β (clone B122). Cell suspensions from bones, muscles and brains of 24-month old wild type mice used as controls were stained in parallel. The percentages of IL-1 $\beta^{(+)}$ Ly6C⁽⁺⁾ macrophages were determined in each compartment and compared between VCP^{R155H/+} heterozygote mice ($n = 8$) and WT mice ($n = 8$). **(F)** The bar graphs represent the means and SD of the percentages of IL-1 $\beta^{(+)}$ Ly6C⁽⁺⁾ macrophages in the muscles, brains, and bones from a group of 8 VCP^{R155H/+} heterozygote mice and 8 WT mice. **(G)** The bar graphs represent the means and SD of the absolute numbers of IL-1 $\beta^{(+)}$ Ly6C⁽⁺⁾ macrophages detected in the muscles, brains, and bones from a group of VCP^{R155H/+} heterozygote mice and WT mice ($n = 8$). Experiments shown are representative of two independently experiments. (*) Indicates $P < 0.05$ when comparing percentages and number of IL-1 $\beta^{(+)}$ F4/80⁽⁺⁾ and IL-1 $\beta^{(+)}$ Ly6C⁽⁺⁾ macrophages in VCP^{R155H/+} heterozygote mice and WT mice using the *Mann-Whitney* test and 2-tails analysis.



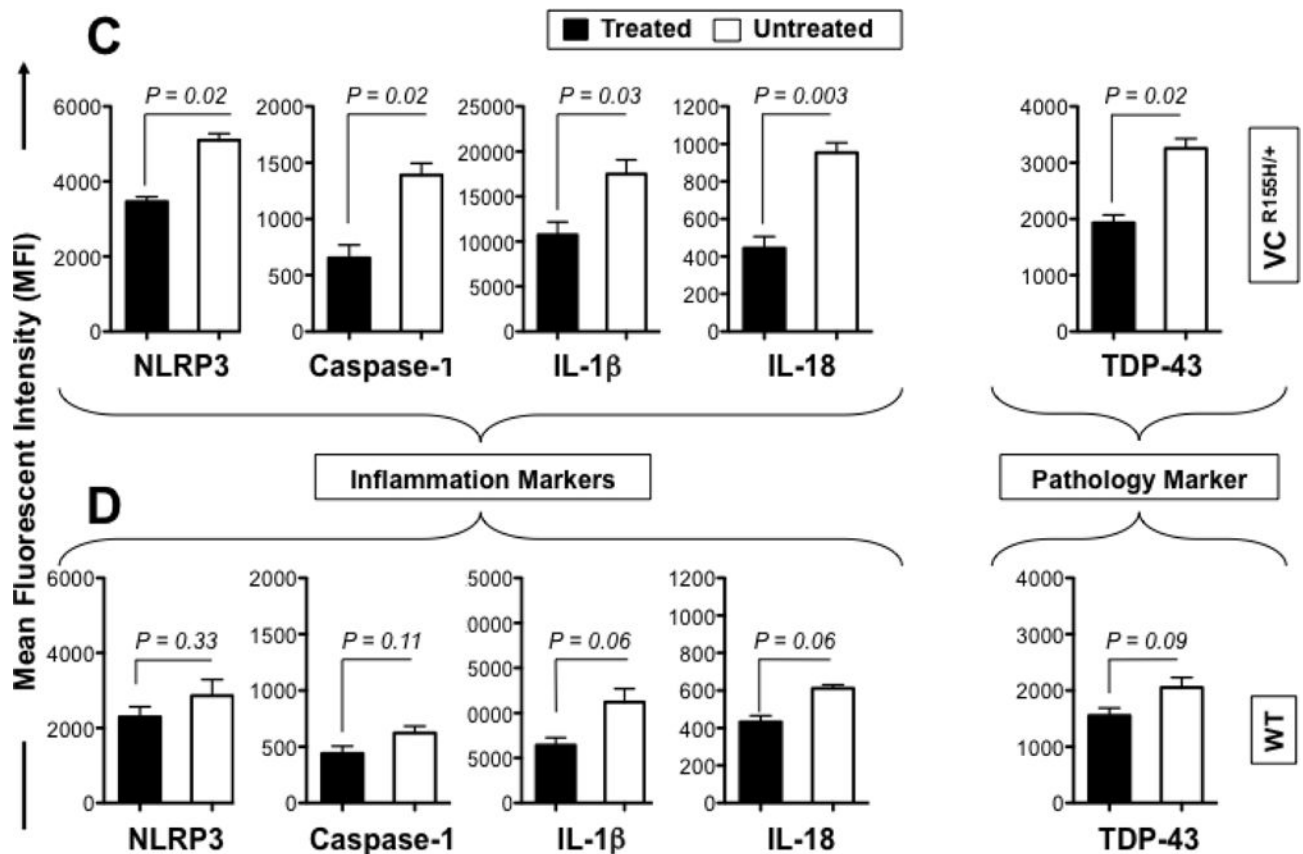
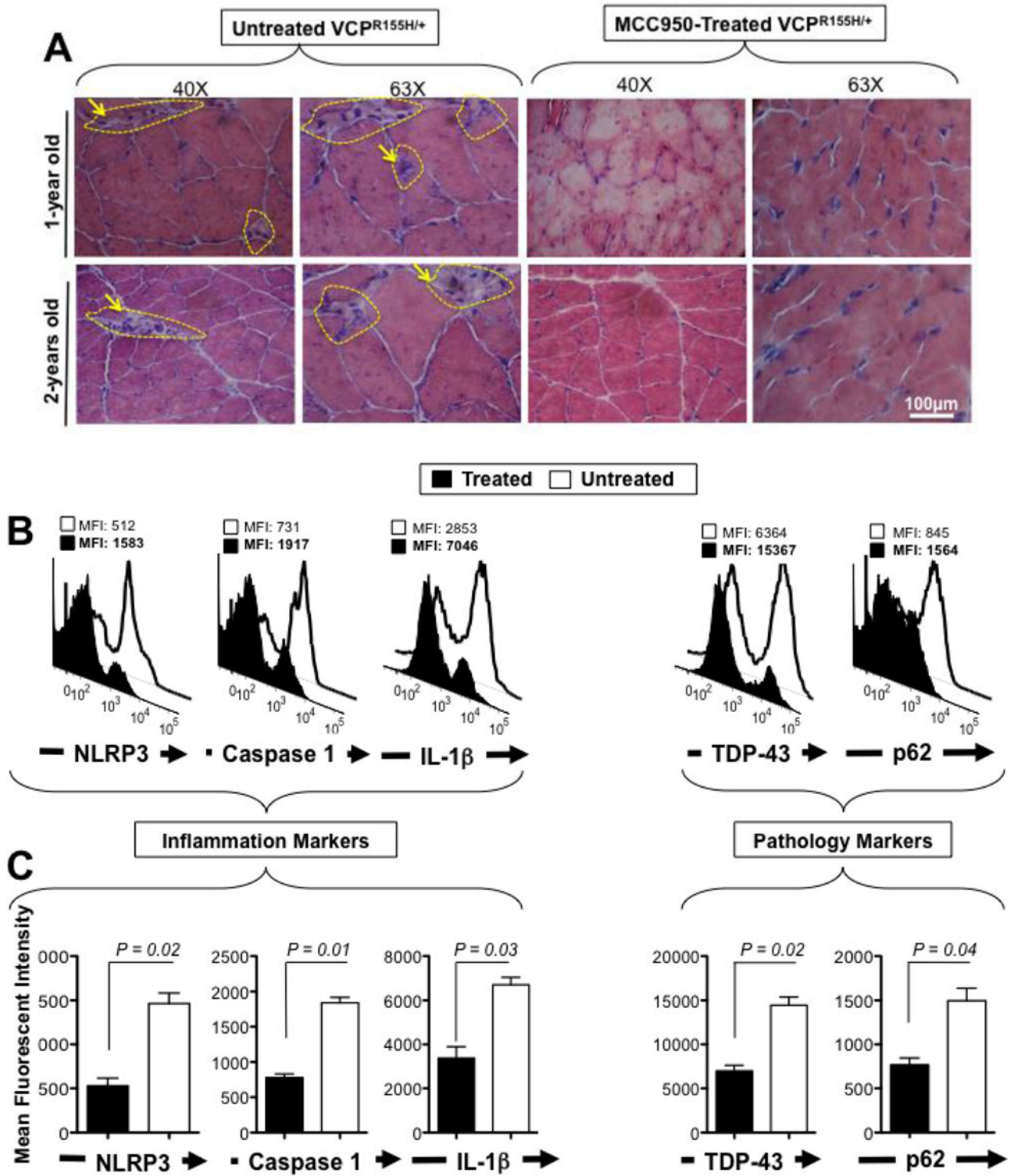


Figure 5. Activation of NLRP3 inflammasome is reversed in myoblasts from VCP^{R155H/+} heterozygote mice following *in vitro* treatment with MCC950 pharmacologic inhibitor Myoblasts were derived from 12-month old VCP^{R155H/+} heterozygotes mice ($n = 8$) and age- and sex-matched healthy mice ($n = 8$, controls). Mouse myoblasts were left untreated (white line) or treated (black line) for 16 hours with 10 μ M MCC950 inhibitor. Treated and untreated myoblasts were stained with mAbs specific to mouse NLRP3, Caspase 1, IL-1 β and IL-18 (markers of inflammasome activation) and then analyzed by flow cytometry, as in Fig. 2. Shown are (A) FACS histograms of markers of the NLRP3 inflammasome activation in myoblasts from VCP^{R155H/+} heterozygote mice (B) and healthy control mice. (C) The bar graphs represent the means and SD of the mean fluorescent intensity (MFI) of each marker (NLRP3, Caspase-1, IL-1 β , IL-18 and TDP-43) in the myoblasts from a group of 8 treated and 8 untreated VCP^{R155H/+} heterozygote mice. (D) The bar graphs represent the means and SD of the mean fluorescent intensity (MFI) of each marker (NLRP3, Caspase-1, IL-1 β , IL-18 and TDP-43) in the myoblasts from a group of 8 treated and 8 untreated WT mice. Experiments shown are representative of two independently experiments. (*) Indicates $P < 0.05$ and (**) indicates $P < 0.01$ when comparing treated and untreated mice using *Mann-Whitney* test and 2-tails analysis.



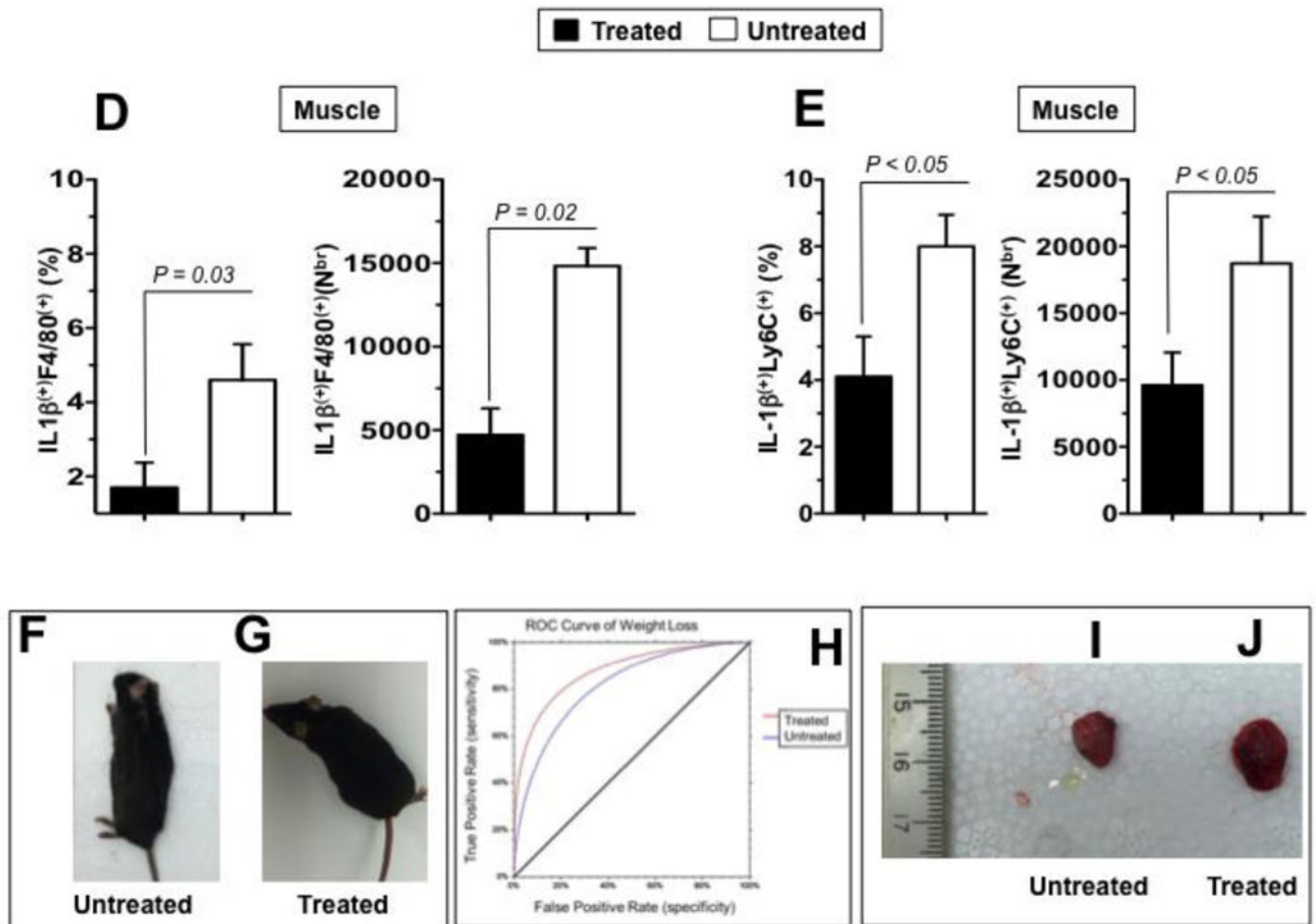


Figure 6. Treatment of with MCC950 inhibitor suppresses of NLRP3 inflammasome activation and ameliorates muscle strength of VCP^{R155H/+} heterozygote mice

Two groups of sex-matched 12-month VCP^{R155H/+} heterozygotes mice ($n = 8$ mice per group) received oral gavage of 30-mg/kg of MCC950 inhibitor for 4 consecutive weeks. Untreated age- and sex-matched VCP^{R155H/+} heterozygotes mice were used as controls. (A) The hematoxylin and eosin sections showing cell infiltrates in muscle of treated vs. Untreated VCP^{R155H/+} heterozygote mice (Magnification at 40× and 63×). As depicted, yellow dotted lines show fibrosis, central nucleation indicating regeneration, and degenerating fibers, and yellow arrows point to persistent neutrophils, macrophages and necrotic myocytes. Quadriceps, brains, and bones were harvested 4 weeks later from untreated and treated mice and stained with mAbs specific to markers of NLRP3 inflammasome activation (NLRP3, Caspase 1, and IL-1β and mAbs specific to markers of pathology TDP-43 and p62/*SQSTM1*) as performed in Figs. 2 and 5. (B) Representative FACS histograms of the levels of markers of inflammasome activation and of pathology (NLRP3, Caspase 1, IL-1β, TDP-43, and P62/*SQSTM1*) detected by flow cytometry from one treated (black line) and untreated (white line) VCP^{R155H/+} heterozygote mice. (C) The bar graphs represent the means and SD of the mean fluorescent intensity (MFI) each marker (NLRP3, Caspase 1, IL-1β, TDP-43, and P62/*SQSTM1*) from a group of 8 treated and 8 untreated VCP^{R155H/+} heterozygotes mice. (*) Indicates $P < 0.05$ when comparing treated and untreated mice using ANOVA test. (D) Percentages (*left graph*) and number (*right*

graph) of F4/80⁽⁺⁾IL-1 β ⁽⁺⁾ macrophages determined in the muscle from treated versus untreated VCP^{R155H/+} heterozygote mice. **(E)** Percentages (*left graph*) and numbers (*right graph*) of IL-1 β ⁽⁺⁾Ly6C⁽⁺⁾ macrophages determined in the muscle from treated versus untreated VCP^{R155H/+} heterozygote mice. **(F and G)** Body size/shape of treated versus untreated VCP^{R155H/+} heterozygote mice, **(H)** ROC curve showing weight loss (red line = treated; blue line = untreated), and **(I and J)** muscle mass loss of fore limb quadriceps observed in untreated versus treated VCP^{R155H/+} heterozygote mice.

Table 1
Grip strength analysis in untreated and MCC950-treated VCPR155H/+ heterozygote mice

Grip strength analysis of 12-month and 18-month old VCPR^{155H/+} animals either untreated or treated with MCC950. *P* < 0.05 indicated statistical significance.

Age	Untreated VCPR ^{155H/+}	MCC950-Treated VCPR ^{155H/+}	<i>P</i> -Value
12 months	40.1 ± 3.2	50.3 ± 4.6	0.045
18 months	41.6 ± 3.9	42.5 ± 2.6	0.087

Author Manuscript

Author Manuscript

Author Manuscript

Author Manuscript